Article

Pregnancy enables antibody protection against intracellular infection

https://doi.org/10.1038/s41586-022-04816-9

Received: 27 June 2021

Accepted: 27 April 2022

Published online: 8 June 2022

Check for updates

John J. Erickson[1,2], Stephanie Archer-Hartmann[3], Alexander E. Yarawsky[4], Jeanette L. C. Miller[4], Stephanie Seveau[5], Tzu-Yu Shao[1], Ashley L. Severance[1], Hilary Miller-Handley[1,6], Yuehong Wu[1], Giang Pham[1], Brian R. Wasik[7], Colin R. Parrish[7], Yueh-Chiang Hu[8], Joseph T. Y. Lau[9], Parastoo Azadi[3], Andrew B. Herr[4] & Sing Sing Way[1]✉

Adaptive immune components are thought to exert non-overlapping roles in antimicrobial host defence, with antibodies targeting pathogens in the extracellular environment and T cells eliminating infection inside cells[1,2]. Reliance on antibodies for vertically transferred immunity from mothers to babies may explain neonatal susceptibility to intracellular infections[3,4]. Here we show that pregnancy-induced post-translational antibody modification enables protection against the prototypical intracellular pathogen *Listeria monocytogenes*. Infection susceptibility was reversed in neonatal mice born to preconceptually primed mothers possessing *L. monocytogenes*-specific IgG or after passive transfer of antibodies from primed pregnant, but not virgin, mice. Although maternal B cells were essential for producing IgGs that mediate vertically transferred protection, they were dispensable for antibody acquisition of protective function, which instead required sialic acid acetyl esterase[5] to deacetylate terminal sialic acid residues on IgG variable-region *N*-linked glycans. Deacetylated *L. monocytogenes*-specific IgG protected neonates through the sialic acid receptor CD22[6,7], which suppressed IL-10 production by B cells leading to antibody-mediated protection. Consideration of the maternal–fetal dyad as a joined immunological unit reveals protective roles for antibodies against intracellular infection and fine-tuned adaptations to enhance host defence during pregnancy and early life.

Infection remains a leading cause of neonatal mortality[8]. Although antibodies broadly defend against infection, they are thought to offer limited protection against pathogens that reside inside cells, which are primarily targeted by T cells[1,2]. Division of labour between adaptive immune components may explain why newborn babies, who rely on vertically transferred maternal antibodies, are especially susceptible to intracellular infections[4]. The intracellular niche is exploited by many pathogens that cause perinatal infection, including the Gram-positive bacterium *L. monocytogenes* (*Lm*), which rapidly gains access to the cell cytoplasm using the pore-forming toxin listerolysin O (LLO), thereafter spreading from the cytoplasm of one cell to another through ActA-mediated actin polymerization[9,10].

Vertically transferred immunity primed by natural infection, vaccination or commensal colonization of mothers dictates the adaptive immune repertoire of neonates[8,11]. Inadequate acquisition of protective maternal antibodies in premature or formula-fed infants increases the risk of infection[12]. However, as protective immunity against *Lm* and other intracellular pathogens has primarily been defined using passive transfer to and from adult recipients[13–15], the relevance to vertically transferred protection of neonates remains uncertain. We used the shared susceptibility to *Lm* infection between human babies and neonatal mice to examine how changes that are unique to the maternal–fetal dyad control immunity against intracellular infection.

Antibodies protect against *Lm* infection

To investigate vertically transferred immunity against intracellular infection, we evaluated the susceptibility of neonatal mice born to preconceptually primed *Lm* immune mothers. To eliminate the possibility of vertically transferred infection, attenuated *Lm* lacking ActA (ΔActA *Lm*), which is rapidly cleared yet retains immunogenicity even in immunocompromised mice[9,10], was used to prime virgin female mice. After infection with virulent *Lm*, neonatal mice born to primed mothers, compared with controls born to naive mothers, possessed elevated anti-*Lm* IgG titres that paralleled enhanced survival and significantly reduced bacterial burdens in the spleen and liver (Fig. 1a–c). Analogous

[1]Department of Pediatrics, Division of Infectious Diseases, Center for Inflammation and Tolerance, Cincinnati Children's Hospital Medical Center, University of Cincinnati School of Medicine, Cincinnati, OH, USA. [2]Department of Pediatrics, Division of Neonatology, Cincinnati Children's Hospital Medical Center, University of Cincinnati School of Medicine, Cincinnati, OH, USA. [3]Complex Carbohydrate Research Center, University of Georgia, Athens, GA, USA. [4]Department of Pediatrics, Division of Immunobiology, Cincinnati Children's Hospital Medical Center, University of Cincinnati School of Medicine, Cincinnati, OH, USA. [5]Department of Microbial Infection and Immunity, Ohio State University, Columbus, OH, USA. [6]Department of Internal Medicine, Division of Infectious Diseases, University of Cincinnati School of Medicine, Cincinnati, OH, USA. [7]Department of Microbiology and Immunology, College of Veterinary Medicine, Cornell University, Ithaca, NY, USA. [8]Department of Pediatrics, Division of Developmental Biology, Cincinnati Children's Hospital Medical Center, University of Cincinnati School of Medicine, Cincinnati, OH, USA. [9]Department of Molecular and Cell Biology, Roswell Park Comprehensive Cancer Center, Buffalo, NY, USA. ✉e-mail: singsing.way@cchmc.org

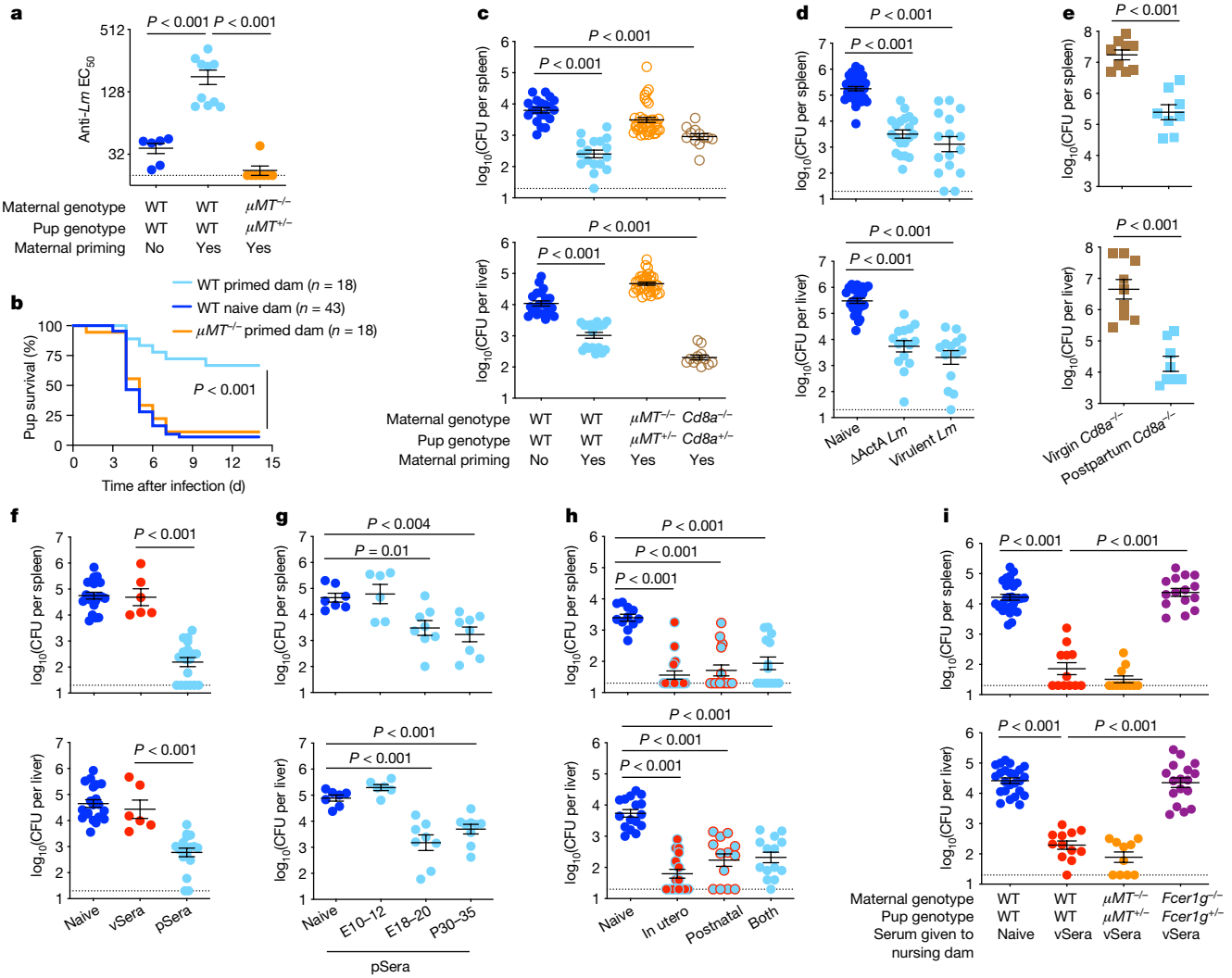

Fig. 1 | Anti-*Lm* antibodies acquire protective function during pregnancy. **a**–**c**, Anti-*Lm* IgG titres (**a**), survival (**b**) and bacterial burdens (**c**) in neonatal mice infected with virulent *Lm* born to WT, $\mu MT^{-/-}$ or $Cd8a^{-/-}$ female mice primed with attenuated ΔActA *Lm* 1 week before mating or naive WT control mice without preconceptual priming. **d**, The bacterial burden in neonatal mice infected with virulent *Lm* born to WT female mice primed with ΔActA *Lm* or virulent *Lm* 3 weeks before mating. **e**, The bacterial burden 3 days after secondary challenge of ΔActA-*Lm*-primed virgin female $Cd8a^{-/-}$ adult mice or preconceptually ΔActA-*Lm*-primed $Cd8a^{-/-}$ female mice 3 weeks postpartum. **f**, The bacterial burden after virulent *Lm* infection in neonatal mice that received sera from ΔActA-*Lm*-primed virgin (vSera) or pregnant mice in late gestation to early postpartum (pSera). **g**, The bacterial burden after virulent *Lm* infection in neonatal mice that received sera from preconceptual ΔActA-*Lm*-primed mice collected at the indicated pregnancy or postpartum time points. **h**, The bacterial burden after virulent *Lm* infection in neonatal mice cross-fostered within 12 h after birth by naive or ΔActA-*Lm*-primed dams. **i**, The bacterial burden after infection with virulent *Lm* in neonatal mice nursed by WT, $\mu MT^{-/-}$ or $Fcer1g^{-/-}$ (FcγR-deficient) mice administered vSera on the day of delivery and 3 days later. Pups were infected with virulent *Lm* 3–4 days after birth. Bacterial burden was enumerated 72 h after infection. For **a**–**i**, each symbol represents an individual mouse. The graphs show data combined from at least 2 independent experiments each with 3–5 mice per group per experiment. Data are mean ± s.e.m. *P* values between key groups were determined using one-way analysis of variance (ANOVA) adjusting for multiple comparisons (**a**, **c**, **d** and **f**–**i**), unpaired *t*-tests (**e**) and log-rank (Mantel–Cox) tests (**b**). The dotted lines show the limit of detection.

experiments evaluating pups born to B-cell-deficient (homozygous for a mutation in *Ighm* ($\mu MT^{-/-}$)) or CD8 T cell deficient ($Cd8a^{-/-}$) primed mothers revealed a requirement for maternal B cells, but not CD8 cells, in vertically transferred immunity against *Lm* infection (Fig. 1a–c). Wild-type (WT) male mice sired pregnancy generating phenotypically WT offspring ($\mu MT^{+/-}$ and $Cd8a^{+/-}$), excluding susceptibility differences from neonatal B or T cell deficiency. Resistance to *Lm* infection was enhanced in pups possessing a higher titre of anti-*Lm* IgG that were born to ΔActA *Lm* primed and boosted mothers (Extended Data Fig. 1a,b). Vertically transferred immunity also occurred with maternal preconceptual virulent *Lm* infection (Fig. 1d) and was specific to *Lm*, as neonatal mice born to dams that were primed with ΔActA *Lm* showed equal susceptibility to the fungal pathogen *Candida albicans* (Extended Data Fig. 1c). Thus, maternal B cells are critical mediators of vertically transferred immunity extending to intracellular infection.

Given these counterintuitive roles for humoral compared with cellular immune components in vertically transferred anti-*Lm* immunity, we verified the importance of CD8 T cells and the non-essential role of B cells for *Lm* protection in primed adult virgin mice[1,2,13–15] (Extended Data Fig. 1d). Interestingly, CD8-mediated immunity could be bypassed by pregnancy, given the significantly reduced *Lm* susceptibility in primed postpartum $Cd8a^{-/-}$ mothers compared with primed virgin females, which each contained similar anti-*Lm* antibody titres (Fig. 1e and Extended Data Fig. 1e). Pregnancy-enabled antibody-mediated protection was confirmed by showing that neonates that were passively transferred sera from *Lm*-primed pregnant and postpartum dams

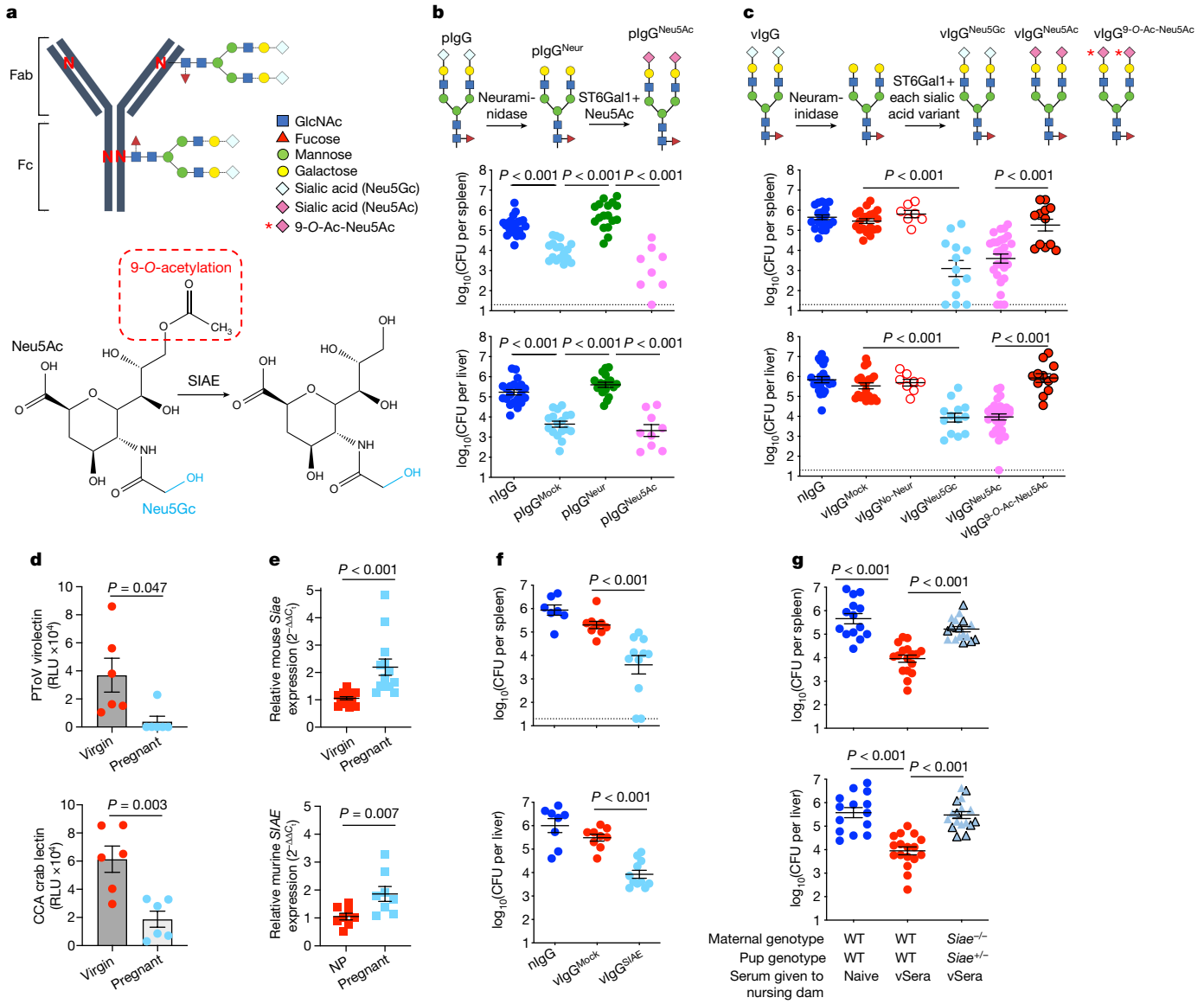

Fig. 2 | SIAE deacetylates anti-*Lm* IgG sialic acid, enabling antibody-mediated protection. a, Schematic of IgG *N*-linked glycosylation, including sialic acid variants and SIAE activity. **b**, IgG from naive (nIgG) or preconceptual ΔActA-*Lm*-primed pregnant/postpartum (pIgG) mice was glycoengineered to remove existing sialic acid with neuraminidase (pIgG^{Neur}) followed by resialylation with ST6Gal1 plus CMP-Neu5Ac (pIgG^{Neu5Ac}) (top). The bacterial burdens after virulent *Lm* infection in neonatal mice after the transfer of the indicated pIgG preparations (bottom). **c**, IgG was recovered from naive (nIgG) or ΔActA-*Lm*-primed virgin (vIgG) mice, treated with neuraminidase and then resialylated with each sialic acid variant using ST6Gal1 plus CMP-sialic acid donors (top). The bacterial burdens after *Lm* infection in neonatal mice after transfer of the indicated vIgG preparations (bottom). **d**, PToV virolectin and CCA lectin detection of 9-*O*-acetyl-Neu5Gc in LLO-specific IgG from virgin compared with pregnant mice. **e**, Relative *Siae* expression in splenocytes from virgin mice and late gestation (E18–20) pregnant mice, or in human peripheral blood mononuclear cells from non-pregnant (NP) versus pregnant women (12–32 weeks gestation). **f**, The bacterial burden after *Lm* infection in neonatal mice that were administered SIAE- or mock-treated vIgG. **g**, The bacterial burden after *Lm* infection in neonatal mice nursed by WT or *Siae*$^{-/-}$ (exon 3 deletion (black outline) and exon 3–4 deletion (no outline)) mice administered vSera on the day of delivery and 3 days later. Pups were infected with virulent *Lm* 3–4 days after birth and, where indicated, 24 h after antibody transfer. Bacterial burden was enumerated 72 h after infection. For **b**–**g**, each symbol represents an individual mouse. The graphs show data combined from at least 2 independent experiments each with 3–5 mice per group per experiment (**b**, **c** and **e**–**g**) or representative data from more than 3 independent experiments (**d**). Data are mean ± s.e.m. *P* values between key groups were determined using one-way ANOVA adjusting for multiple comparisons (**b**, **c**, **f**, **g**) or unpaired *t*-tests (**d**, **e**). The dotted lines show the limit of detection.

(pSera), but not sera from primed virgin mice (vSera), had reduced susceptibility to *Lm* despite having a reduced antibody titre (Fig. 1f and Extended Data Fig. 2a). Protective antibodies emerged in late pregnancy; sera collected from preconceptually primed mice in late gestation (embryonic day 18–20 (E18–20)) or postpartum (P30–35) were similarly efficacious, whereas sera from mid-gestation (E10–12) donor mice were non-protective (Fig. 1g). Cross-fostering studies demonstrated the transfer of protective *Lm*-specific IgG regardless of in utero or postnatal acquisition through breastfeeding with similarly reduced neonatal *Lm* susceptibility (Fig. 1h and Extended Data Fig. 2b).

We next took advantage of the efficient breastmilk transfer of maternal antibodies to further investigate whether pregnancy enabled protection through de novo antibody production or post-translational modification of pre-existing antibodies. Notably, anti-*Lm* IgG in vSera became protective when indirectly transferred to pups through WT or *μMT*$^{-/-}$ nursing dams, dissociating protective antibody conversion

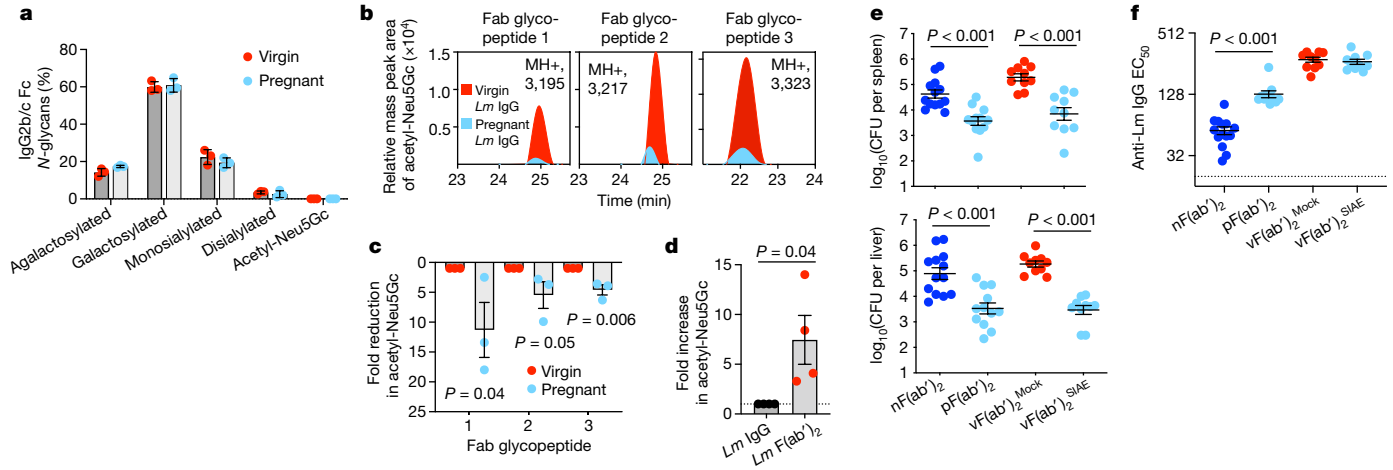

Fig. 3 | Acetylated sialic acid localizes to Fab *N*-glycans. a, The percentage of conserved IgG2 Fc *N*-glycan sites with each indicated glycoform. **b**, Relative mass peak area for acetyl-Neu5Gc determined by MS/MS oxonium ion filtering analysis of three unique Fab glycopeptides from *Lm*-specific IgG purified from virgin or pregnant mice. MH+, protonated molecular mass. **c**, The fold-reduction in acetyl-Neu5Gc for each Fab glycopeptide in *Lm*-specific IgG (from **b**) of pregnant compared with virgin mice. **d**, The fold increase in acetyl-Neu5Gc after pepsin treatment for Fab glycopeptides relative to untreated full-length IgG. **e**,**f**, The bacterial burdens (**e**) and anti-*Lm* $F(ab')_2$ titres (**f**) after virulent *Lm* infection in neonatal mice transferred pepsin-treated IgG from naive mice ($nF(ab')_2$), pregnant/postpartum *Lm*-primed mice ($pF(ab')_2$) or virgin *Lm*-primed mice ($vF(ab')_2$) treated with SIAE to remove acetylation from sialic acid residues. Pups were infected with virulent *Lm* 4 days after birth, 24 h after $F(ab')_2$ transfer; bacterial burden was enumerated 72 h after infection. MS experiments were performed 3–4 times using purified IgG pooled from virgin or pregnant mice and data from each replicate experiment are shown (**a**–**d**). For infection and anti-*Lm* titres in **e** and **f**, each symbol represents an individual mouse, with graphs showing data combined from at least 2 independent experiments each with 3–5 mice per group per experiment. Data are mean ± s.e.m. *P* values between key groups are shown as determined using one-way ANOVA adjusting for multiple comparisons (**e** and **f**) or unpaired *t*-tests (**c** and **d**).

from maternal B cells (Fig. 1i and Extended Data Fig. 2c). However, maternal Fcγ receptors (FcγRs), which are broadly required for leukocyte-mediated antibody effector functions[16,17], were essential, as pups nursed by *Fcer1g*$^{-/-}$ (FcγR-deficient) dams that were passively transferred vSera remained susceptible despite anti-*Lm* IgG transfer through the breastmilk (Fig. 1i and Extended Data Fig. 2c). WT males again sired pregnancy generating phenotypically WT (*μMT*$^{+/-}$ and *Fcer1g*$^{+/-}$) offspring. Antibody acquisition of protective function requiring maternal FcγR was recapitulated in vitro, as incubating vSera with splenocytes from pregnant WT mice, but not pregnant *Fcer1g*$^{-/-}$ mice, enabled protection when passively transferred to neonatal recipients (Extended Data Fig. 2d). Thus, although maternal B cells are essential for producing antibodies that mediate vertically transferred immunity, they are dispensable for pregnancy-induced acquisition of protective function, which instead relies on the modification of pre-existing anti-*Lm* IgG and FcγR-bearing maternal cells.

Pregnancy deacetylates IgG sialic acid

IgG purified from *Lm*-primed virgin (vIgG) and preconceptually primed pregnant/postpartum (pIgG) mice was compared to determine the molecular features that are responsible for discordant protection against intracellular infection. Pregnancy altered neither the overall titre nor the level of individual antibody isotypes with specificity to *Lm* bacteria or purified LLO protein, with predominant accumulation of IgG2 (Extended Data Fig. 3a,b). vIgG and pIgG similarly reduced LLO-induced haemolysis, indicating no difference in functional neutralization (Extended Data Fig. 3c). vIgG and pIgG binding to a panel of carbohydrate-specific lectins showed similar patterns of *N*-linked glycosylation, an important post-translational IgG modification, with predominant terminal α2,6-linked sialic acid (Fig. 2a and Extended Data Fig. 3d). *Sambucus nigra* agglutinin (SNA) lectin fractionization, which preferentially binds to IgG with sialylated Fab-region *N*-glycans[18], revealed that >90% of anti-*Lm* IgG contains sialic acid (Extended Data Fig. 3e,f).

The functional importance of sialic acid was evaluated by neuraminidase digestion, demonstrating that desialylation completely abolished pIgG-mediated protection against neonatal *Lm* infection (Fig. 2b). Reciprocally, protection was fully restored by ST6 β-galactosidase α2,6-sialyltransferase 1 (ST6Gal1) addition of sialic acid in the form of acetylneuraminic acid (Neu5Ac) (Fig. 2b and Extended Data Fig. 3g,h). Interestingly, vIgG did not acquire protective function by directly adding Neu5Ac without neuraminidase pretreatment (Fig. 2c), suggesting that molecular variants of sialic acid[19] could be responsible for the differential protection between vIgG and pIgG. Porcine torovirus (PToV) haemagglutinin esterase lectin with specificity for 9-*O*-acetylated sialic acid[20,21] displayed substantially reduced binding to LLO-specific IgG from pregnant compared with virgin mice (Fig. 2d and Extended Data Fig. 3k). *Cancer antennarius* (CCA) lectin with specificity for 9-*O*- and 4-*O*-linked acetylation[22] showed similar differences (Fig. 2d), whereas neither vIgG nor pIgG bound to mouse hepatitis virus haemagglutinin esterase lectin with 4-*O*-acetylated sialic acid specificity[20,21], indicating selective 9-*O*-acetylation of sialic acid on *Lm*-specific IgG from virgin compared with pregnant mice. Importantly, vIgG acquired protective function after replacement of native sialic acid with Neu5Ac (the predominant human variant due to CMAH inactivation[23]) or glycolylneuraminic acid (Neu5Gc; the predominant murine sialic acid[24]), but not 9-*O*-acetylated sialic acid (9-*O*-Ac-Neu5Ac) (Fig. 2c). Similar titres of anti-*Lm* IgG were transferred to neonates, and staining with multiple lectins confirmed precise sialylation with each glycoform (Extended Data Fig. 3i–k). Thus, 9-*O*-acetylation of *N*-glycan terminal sialic acid residues renders antibodies non-protective against *Lm* infection.

Sialic acid acetyl esterase (SIAE) removes 9-*O*-acetylation from sialic acid (Fig. 2a). *SIAE* polymorphisms are linked to autoimmunity and disregulated expression associated with pregnancy complications[5,25]. We found pregnancy-induced upregulation of SIAE in leukocytes of both mice and women (Fig. 2e), suggesting conserved regulation of sialic acid deacetylation during pregnancy. Importantly, SIAE removal of 9-*O*-acetylation from vIgG, confirmed by PToV lectin staining (Extended Data Fig. 3k), reduced bacterial burdens and enhanced survival after transfer into neonatal mice (Fig. 2f and Extended Data Fig. 4a,b).

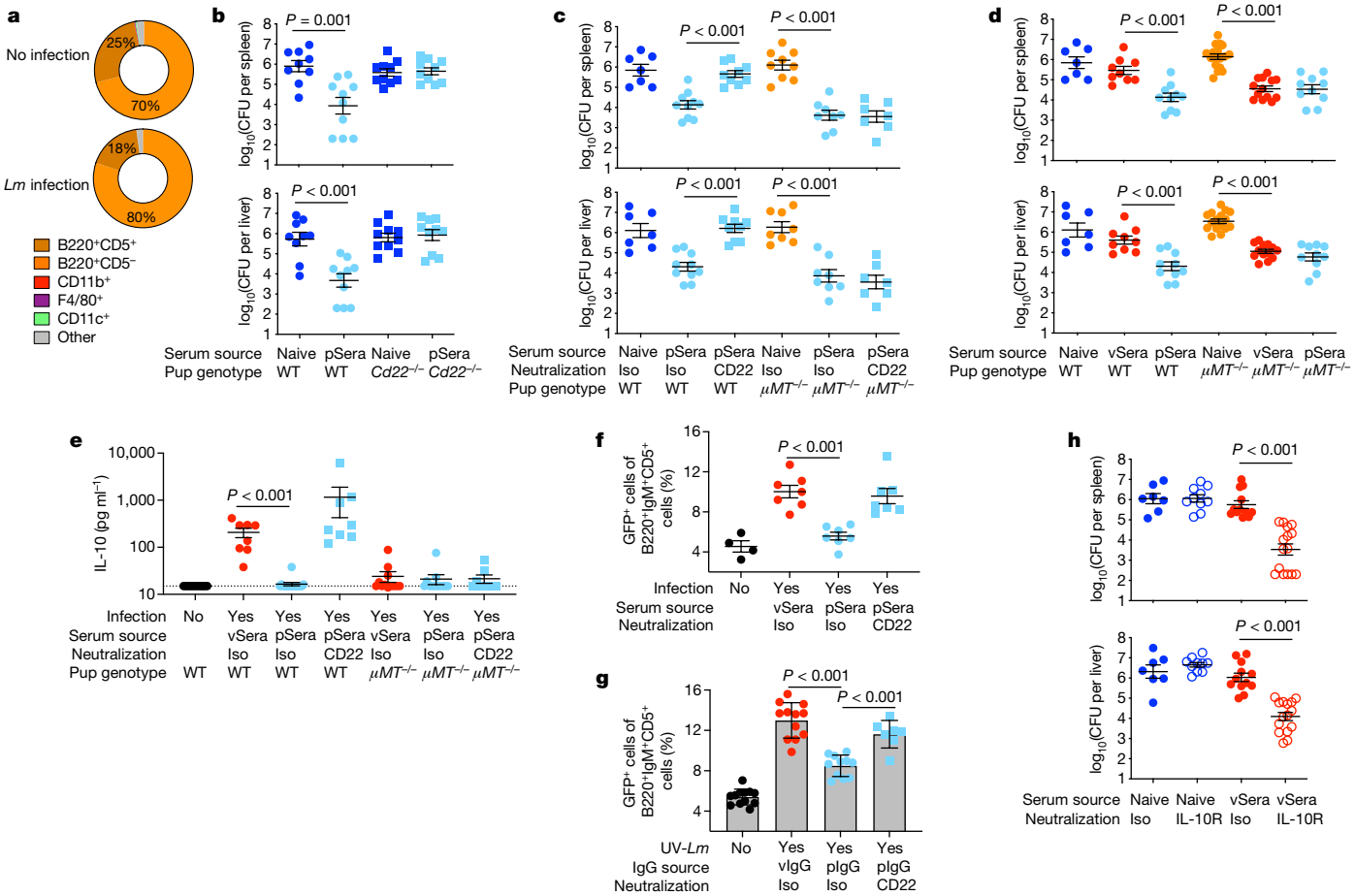

Fig. 4 | Deacetylated anti-*Lm* antibodies protect through CD22-mediated suppression of B cell IL-10 production. a, $CD22^+$ cell distribution among neonatal splenocytes 72 h after *Lm* infection compared with uninfected controls. **b**, The bacterial burden after *Lm* infection of WT or CD22-deficient neonatal mice transferred sera from ΔActA-*Lm*-primed pregnant/postpartum (pSera) or naive mice. **c**, The bacterial burden after *Lm* infection of WT or $\mu MT^{-/-}$ neonates that were administered pSera or naive sera, along with anti-CD22 or isotype control (Iso) antibodies. **d**, The bacterial burden after *Lm* infection of WT or $\mu MT^{-/-}$ neonates that were administered with sera from ΔActA-*Lm*-primed virgin mice (vSera), pSera or naive sera. **e**, Serum IL-10 levels 72 h after *Lm* infection in WT or $\mu MT^{-/-}$ neonates that were administered with vSera or pSera, plus anti-CD22 antibodies. **f**, GFP expression in $B220^+IgM^+CD5^+$ splenocytes 72 h after *Lm* infection in neonatal IL-10–eGFP reporter mice that were administered with vSera or pSera, plus anti-CD22 antibodies, compared with uninfected mice. **g**, GFP expression by $B220^+IgM^+CD5^+$ splenocytes from IL-10–eGFP neonates stimulated with inactivated *Lm* (UV-*Lm*) in the presence of vIgG or pIgG, plus anti-CD22 antibodies. **h**, The bacterial burden after *Lm* infection in neonates administered with vSera or naive sera, along with anti-IL-10R antibodies or isotype control antibodies. Neonatal mice were infected with virulent *Lm* 3–4 days after birth, 24 h after antibody transfer; bacterial burden was enumerated 72 h after infection. The pie charts in **a** show representative data from 1 out of 3 independent experiments, averaged across 5 mice per group. For **b**–**h**, each symbol represents the data from an individual mouse with graphs showing data combined from at least 3 independent experiments with 3–5 mice per group per experiment (**b**–**f** and **h**) or cells in an individual well under unique stimulation conditions combined from 4–5 independent experiments (**g**). For **b**–**h**, data are mean ± s.e.m. *P* values between groups in **b**–**h** were determined by one-way ANOVA adjusting for multiple comparisons. The dotted line in **e** shows the limit of detection.

The protective potency of pIgG was not further enhanced by SIAE treatment (Extended Data Fig. 4c,d), indicating that deacetylation was optimal during pregnancy. Two independently generated strains of SIAE-deficient mice (exon 3 and exon 3–4 deletion) each verified that maternal SIAE is essential for converting non-protective acetylated IgG present in vSera to the protective deacetylated form (Fig. 2g and Extended Data Fig. 4e). Comparatively, retained protective conversion of vSera in *St6gal1*$^{-/-}$ mice indicates that anti-*Lm* IgG is not desialylated and then resialylated (Extended Data Fig. 4f). Thus, SIAE-mediated sialic acid deacetylation of antibodies during pregnancy enables their protective function against intracellular infection.

Acetylation localizes to the Fab region

Tandem mass spectrometry (MS/MS) analysis of purified *Lm*-specific IgG from virgin and pregnant mice was performed to confirm sialic acid acetylation on the basis of oxonium ion signatures[26] (Extended Data Fig. 5a–c). Glycopeptide mapping revealed the absence of acetylation on conserved Fc-region *N*-linked glycans, with only 20–25% of IgG2 Fc containing any sialic acid, all in the form of Neu5Gc (Fig. 3a and Extended Data Fig. 6). Instead, biantennary *N*-glycans containing acetylated Neu5Gc (acetyl-Neu5Gc) were identified in three unique glycopeptides, each demonstrating a 42 Da mass increase over Neu5Gc, corresponding to the addition of a single acetyl group and excluding derivation from other acetylated biomolecules (Extended Data Fig. 7). Importantly, these glycopeptides from pregnant compared with virgin *Lm*-specific IgG contain five to tenfold less acetyl-Neu5Gc (Fig. 3b,c), consistent with previous results using PToV and CCA lectin staining for 9-*O*-acetyl-Neu5Gc (Fig. 2d and Extended Data Fig. 3j,k).

We reasoned that 9-*O*-acetylation localizes to terminal sialic acid residues in the polymorphic Fab variable region as acetylated sialic acid

was neither present on the conserved Fc glycosylation site nor found to originate from variable-region immunoglobulin genes containing germline-encoded *N*-linked glycosylation sites[27]. Fab glycosylation was confirmed on the basis of retained α2,6-linked sialic acid and diminished α1,6-linked fucose on *Lm*-specific $F(ab')_2$ fragments (Extended Data Fig. 8a,b), a lectin blot demonstrating α2,6-linked sialic acid on the ~100 kDa $F(ab')_2$ fragments (Extended Data Fig. 8c), and the increased ratio of acetylated to non-acetylated Neu5Gc on *Lm*-specific $F(ab')_2$ fragments compared with full length IgG determined by MS (Fig. 3d). The functional consequences of Fab 9-*O*-acetylation were verified by showing that pIgG-derived $F(ab')_2$ fragments, as well as SIAE-deacetylated vIgG-derived $F(ab')_2$ fragments, each substantially reduced susceptibility to *Lm* infection (Fig. 3e,f). Antibodies from pregnant mice retained protection in anti-FcγR antibody-treated and complement-deficient mice (Extended Data Fig. 8d–f), reaffirming that Fc-mediated functions in neonates are dispensable. Thus, pregnancy expands antibody-mediated protection against intracellular infection through sialic acid deacetylation at the IgG Fab variable region.

CD22-dependent inhibition of B10 cells

As 9-*O*-acetylation masks sialylated ligands for the Siglec CD22, which is primarily expressed by B lymphocytes and blunts their activation[6,7,23,28], we investigated whether pregnancy-deacetylated IgG stimulates CD22-dependent inhibition of B cells. In agreement, ≥95% of $CD22^+$ cells were B lymphocytes (both $B220^+CD5^+$ B-1a cells and $B220^+CD5^-$ cells) in naive and *Lm*-infected neonates (Fig. 4a). CD22 was essential for pSera protection, shown using CD22-deficient mice or WT mice administered with CD22-neutralizing antibodies (Fig. 4b and Extended Data Fig. 9a–c). By contrast, CD22 neutralization failed to override pSera protection in $\mu MT^{-/-}$ pups (Fig. 4c), confirming the importance of CD22 expression by B cells. Given the lower affinity of Neu5Ac-containing ligands compared with Neu5Gc-containing ligands for murine CD22[29,30], the dependence on this Siglec for protection by vIgG engineered to express Neu5Ac was confirmed using both CD22-deficient mice and neutralizing antibodies (Extended Data Fig. 9d,e). Furthermore, vSera, which provides no defence in WT mice, efficiently protected $\mu MT^{-/-}$ pups (lacking all B cells) and $Cd19^{-/-}$ pups (lacking only B-1a cells[31,32]), confirming B cell suppression of the protective function of anti-*Lm* antibodies (Fig. 4d and Extended Data Fig. 9f–h).

B lymphocyte subsets producing the immune-suppressive cytokine IL-10 enhance *Lm* susceptibility[33–35]. In agreement, *Lm* induced high serum IL-10 levels in WT, but not $\mu MT^{-/-}$, pups treated with vSera, whereas IL-10 in WT mice was substantially reduced after administration of pSera and reversed by CD22 neutralization (Fig. 4e). The use of IL-10 reporter (Vert-X) mice verified the activation of $B220^+IgM^+CD5^+$ IL-10-producing B cells (B10 cells)[31,32], which exhibited CD22-dependent suppression by pSera (Fig. 4f and Extended Data Fig. 10a). Neonatal B10 cell stimulation in vitro by inactivated *Lm* demonstrated similar CD22-dependent inhibition by pIgG, but not by vIgG (Fig. 4g and Extended Data Fig. 10b,c). Collectively, these results highlight an essential role for CD22 in deacetylated anti-*Lm* IgG suppression of neonatal B10 cells. Importantly, pIgG specifically repressed *Lm* activation of B10 cells as it had no effect on agonistic stimulation through TLR2—the main receptor that is required for innate *Lm* sensing[36] (Extended Data Fig. 10d). The in vivo necessity of IL-10 in overriding protection by anti-*Lm* IgG was confirmed using IL-10 receptor blockade, which enabled protection by vSera (Fig. 4h and Extended Data Fig. 10e), phenocopying results observed in $\mu MT^{-/-}$ and $Cd19^{-/-}$ pups (Fig. 4d and Extended Data Fig. 9f). Thus, the absence of IL-10 or inhibitory B lymphocytes bypasses the functional impairment of acetylated virgin anti-*Lm* IgG, whereas pregnancy deacetylates antibodies enabling CD22-mediated inhibition of B10 cells, enabling protective immunity against *Lm* intracellular infection.

Discussion

The foundational immunological tenet that humoral and cell-mediated adaptive immunity have non-overlapping functions is based largely on *Lm* infection experiments demonstrating that convalescent serum from mice with resolved infection cannot transfer protection to naive recipient mice, whereas protection is readily transferred with donor splenocytes containing T cells[1,2,13–15]. However, these passive transfer studies exclusively using virgin adult animals probably have limited relevance to the unique susceptibility of newborn babies relying on vertically transferred immunity. By considering the maternal–fetal dyad as a joined immunological unit, and the only biological context in which immune components are naturally transferred between individuals, protective roles for *Lm*-specific antibodies are revealed. The expanded scope of antibody-mediated protection is probably especially important during the neonatal period when T-cell-mediated immunity is immature.

A key distinction for *Lm*-primed IgG is the ability to become protective after deacetylation of *N*-glycan sialic acid. Protection occurred despite low-level vertical transfer of polyclonal maternal antibodies, therefore operating through mechanisms that are distinct from those previously shown for neutralizing anti-LLO monoclonal antibody clones that offered protection only at very high titres[37]. Indeed, both in vivo pregnancy and ex vivo enzymatically deacetylated IgG protects against *Lm* through Fab-region sialic acid interactions with the Siglec CD22, which negatively regulates B cell transmembrane signalling through BCR and TLRs by recruitment of the intracellular phosphatases SHP-1 and SHIP[6,7,23]. Antibodies containing sialylated *N*-glycans have previously been shown to bind to CD22 on B cells[38,39]. We demonstrate that anti-*Lm* IgG engineered to express either Neu5Ac or Neu5Gc is protective, despite the lower affinity of Neu5Ac relative to Neu5Gc for murine CD22 binding[29,30]. Thus, engagement with sialylated antibodies probably relies on CD22 clustering to increase avidity, especially given CD22 reorganization near the BCR during B cell activation[40]. Importantly, CD22 binding to sialylated ligands is uniformly silenced by acetylation[28], consistent with our results demonstrating that both anti-*Lm* IgG from virgin mice and glycoengineered IgG expressing 9-*O*-acetylated sialic acid are non-protective.

We also show that CD22 selectively inhibits IL-10 production by B cells, which promote *Lm* susceptibility[33–35]. B10 cells are a regulatory subset of B-1a cells that are activated through BCR or TLR interactions[31], and our findings of reduced IL-10 production by deacetylated IgG are consistent with CD22 inhibition of both of these activating receptors[6,41]. *Lm*-specific IgG may bridge activating B10 receptors and CD22 through bivalent IgG simultaneously binding *Lm* and CD22 through deacetylated Fab sialic acid (Extended Data Fig. 10f). Thus, a key adaptation used by *Lm* to evade antibodies is through the activation of B10 cells, as IL-10 suppresses bactericidal activity in macrophages and other antigen-presenting cells[31,32,35]. These results fundamentally expand the mechanisms of antibody-mediated protection to include intracellular pathogens, which were previously thought to rely primarily on extracellular neutralization or Fc receptor binding[42].

Our results also raise important questions about the immunological consequences of sialic acid deacetylation. *SIAE* polymorphisms have been linked to autoimmune disorders, including rheumatoid arthritis and type I diabetes mellitus[5]. Moreover, *CD22* polymorphisms are associated with systemic lupus erythematosus[43]. These observations in addition to our own data suggest that high-affinity self-reactive antibody clones may be acetylated as a means to prevent autoimmunity through decreased CD22 binding, at the expense of antimicrobial immunity. Sialic acid acetylation also reduces the activity of human neuraminidases[44], which may fine-tune antibody half-life and optimize embryogenesis, as forced expression of sialic-acid-deacetylating enzymes in mice is associated with tissue-specific developmental defects[45]. Suppressed expansion of maternal B cells with fetal specificity by CD22

during murine pregnancy[46], and the increased expression of placental SIAE during human pregnancy complications such as pre-eclampsia[25], together suggest that modulation of sialic acid acetylation promotes fetal tolerance. Acetylated sialic acid is also the target for several viral attachment proteins[20], and SIAE upregulation during pregnancy may therefore decrease infection susceptibility. Important areas for future study include evaluating how SIAE and sialic acid receptors control development and, reciprocally, how the expression of these molecules is developmentally regulated.

Despite these pregnancy-induced antibody modifications, neonatal susceptibility to intracellular infections may reflect inadequate maternal pathogen exposure, especially considering the serotype diversity of common intracellular pathogens. For example, congenital cytomegalovirus infection risk is around 20-fold increased for women with primary infection compared with secondary infection during pregnancy[47], and especially increased by maternal reinfection with a serologically distinct strain of cytomegalovirus[48]. Similarly, resistance to herpes simplex virus in neonates is associated with maternal type-specific antibodies[49]. For *Lm*, the relatively high seroprevalence in women[50], together with the expanded range of protection by *Lm*-specific antibodies that we demonstrate, probably explains the disproportionately small incidence of neonatal infection. In the broader context, consideration of the maternal–fetal dyad as a joined immunological unit reveals protective roles for antibodies against intracellular infection[8,42], highlighting precise fine-tuning of host defences to mitigate vulnerability during pregnancy and in early life.

Online content

Any methods, additional references, Nature Research reporting summaries, source data, extended data, supplementary information, acknowledgements, peer review information; details of author contributions and competing interests; and statements of data and code availability are available at https://doi.org/10.1038/s41586-022-04816-9.

1. Collins, F. M. Cellular antimicrobial immunity. *CRC Crit. Rev. Microbiol.* **7**, 27–91 (1978).
2. Mackaness, G. B. Resistance to intracellular infection. *J. Infect. Dis.* **123**, 439–445 (1971).
3. Albrecht, M. & Arck, P. C. Vertically transferred immunity in neonates: mothers, mechanisms and mediators. *Front. Immunol.* **11**, 555 (2020).
4. Robbins, J. R. & Bakardjiev, A. I. Pathogens and the placental fortress. *Curr. Opin. Microbiol.* **15**, 36–43 (2012).
5. Surolia, I. et al. Functionally defective germline variants of sialic acid acetylesterase in autoimmunity. *Nature* **466**, 243–247 (2010).
6. Clark, E. A. & Giltiay, N. V. CD22: a regulator of innate and adaptive B Cell responses and autoimmunity. *Front. Immunol.* **9**, 2235 (2018).
7. Mahajan, V. S. & Pillai, S. Sialic acids and autoimmune disease. *Immunol. Rev.* **269**, 145–161 (2016).
8. Kollmann, T. R., Marchant, A. & Way, S. S. Vaccination strategies to enhance immunity in neonates. *Science* **368**, 612–615 (2020).
9. Chávez-Arroyo, A. & Portnoy, D. A. Why is *Listeria monocytogenes* such a potent inducer of CD8$^+$ T-cells? *Cell Microbiol.* **22**, e13175 (2020).
10. Radoshevich, L. & Cossart, P. *Listeria monocytogenes*: towards a complete picture of its physiology and pathogenesis. *Nat. Rev. Microbiol.* **16**, 32–46 (2018).
11. Marchant, A. et al. Maternal immunisation: collaborating with mother nature. *Lancet Infect. Dis.* **17**, e197–e208 (2017).
12. Fouda, G. G., Martinez, D. R., Swamy, G. K. & Permar, S. R. The Impact of IgG transplacental transfer on early life immunity. *Immunohorizons* **2**, 14–25 (2018).
13. Kaufmann, S. H., Hug, E. & De Libero, G. *Listeria monocytogenes*-reactive T lymphocyte clones with cytolytic activity against infected target cells. *J. Exp. Med.* **164**, 363–368 (1986).
14. Bishop, D. K. & Hinrichs, D. J. Adoptive transfer of immunity to *Listeria monocytogenes*. The influence of in vitro stimulation on lymphocyte subset requirements. *J Immunol.* **139**, 2005–2009 (1987).
15. Mielke, M. E., Ehlers, S. & Hahn, H. T-cell subsets in delayed-type hypersensitivity, protection, and granuloma formation in primary and secondary *Listeria* infection in mice: superior role of Lyt-2$^+$ cells in acquired immunity. *Infect. Immun.* **56**, 1920–1925 (1988).
16. Bruhns, P. & Jönsson, F. Mouse and human FcR effector functions. *Immunol. Rev.* **268**, 25–51 (2015).
17. Anthony, R. M., Wermeling, F. & Ravetch, J. V. Novel roles for the IgG Fc glycan. *Ann. N. Y. Acad. Sci.* **1253**, 170–180 (2012).
18. van de Bovenkamp, F. S., Hafkenscheid, L., Rispens, T. & Rombouts, Y. The emerging importance of IgG Fab glycosylation in immunity. *J. Immunol.* **196**, 1435–1441 (2016).
19. Traving, C. & Schauer, R. Structure, function and metabolism of sialic acids. *Cell. Mol. Life Sci.* **54**, 1330–1349 (1998).
20. Langereis, M. A. et al. Complexity and diversity of the mammalian sialome revealed by nidovirus virolectins. *Cell Rep.* **11**, 1966–1978 (2015).
21. Srivastava, S. et al. Development and applications of sialoglycan-recognizing probes (SGRPs) with defined specificities: exploring the dynamic mammalian sialoglycome. Preprint at *bioRxiv* https://doi.org/10.1101/2021.05.28.446202 (2021).
22. Ravindranath, M. H., Higa, H. H., Cooper, E. L. & Paulson, J. C. Purification and characterization of an *O*-acetylsialic acid-specific lectin from a marine crab *Cancer antennarius*. *J. Biol. Chem.* **260**, 8850–8856 (1985).
23. Crocker, P. R., Paulson, J. C. & Varki, A. Siglecs and their roles in the immune system. *Nat. Rev. Immunol.* **7**, 255–266 (2007).
24. Krištić, J. et al. Profiling and genetic control of the murine immunoglobulin G glycome. *Nat. Chem. Biol.* **14**, 516–524 (2018).
25. Tsai, S. et al. Transcriptional profiling of human placentas from pregnancies complicated by preeclampsia reveals disregulation of sialic acid acetylesterase and immune signalling pathways. *Placenta* **32**, 175–182 (2011).
26. Medzihradszky, K. F., Kaasik, K. & Chalkley, R. J. Characterizing sialic acid variants at the glycopeptide level. *Anal. Chem.* **87**, 3064–3071 (2015).
27. Melo-Braga, M. N., Carvalho, M. B., Emiliano, M. C., Ferreira & Felicori, L. F. New insights of glycosylation role on variable domain of antibody structures. Preprint at *bioRxiv* https://doi.org/10.1101/2021.04.11.439351 (2021).
28. Sjoberg, E. R., Powell, L. D., Klein, A. & Varki, A. Natural ligands of the B cell adhesion molecule CD22 beta can be masked by 9-O-acetylation of sialic acids. *J. Cell Biol.* **126**, 549–562 (1994).
29. Blixt, O., Collins, B. E., van den Nieuwenhof, I. M., Crocker, P. R. & Paulson, J. C. Sialoside specificity of the siglec family assessed using novel multivalent probes: identification of potent inhibitors of myelin-associated glycoprotein. *J. Biol. Chem.* **278**, 31007–31019 (2003).
30. Brinkman-Van der Linden, E. C. et al. Loss of *N*-glycolylneuraminic acid in human evolution. Implications for sialic acid recognition by siglecs. *J. Biol. Chem.* **275**, 8633–8640 (2000).
31. Tedder, T. F. B10 cells: a functionally defined regulatory B cell subset. *J. Immunol.* **194**, 1395–1401 (2015).
32. Yanaba, K. et al. A regulatory B cell subset with a unique CD1d^{hi}CD5$^+$ phenotype controls T cell-dependent inflammatory responses. *Immunity* **28**, 639–650 (2008).
33. Horikawa, M. et al. Regulatory B cell (B10 Cell) expansion during *Listeria* infection governs innate and cellular immune responses in mice. *J. Immunol.* **190**, 1158–1168 (2013).
34. Lee, C. C. & Kung, J. T. Marginal zone B cell is a major source of Il-10 in *Listeria monocytogenes* susceptibility. *J. Immunol.* **189**, 3319–3327 (2012).
35. Liu, D. et al. IL-10-dependent crosstalk between murine marginal zone B cells, macrophages, and CD8α. *Immunity* **51**, 64–76 (2019).
36. Torres, D. et al. Toll-like receptor 2 is required for optimal control of *Listeria monocytogenes* infection. *Infect. Immun.* **72**, 2131–2139 (2004).
37. Edelson, B. T., Cossart, P. & Unanue, E. R. Cutting edge: paradigm revisited: antibody provides resistance to Listeria infection. *J. Immunol.* **163**, 4087–4090 (1999).
38. Séïté, J. F. et al. IVIg modulates BCR signaling through CD22 and promotes apoptosis in mature human B lymphocytes. *Blood* **116**, 1698–1704 (2010).
39. Adachi, T. et al. CD22 serves as a receptor for soluble IgM. *Eur. J. Immunol.* **42**, 241–247 (2012).
40. Müller, J. et al. CD22 ligand-binding and signaling domains reciprocally regulate B-cell Ca2$^+$ signaling. *Proc. Natl Acad. Sci. USA* **110**, 12402–12407 (2013).
41. Kawasaki, N., Rademacher, C. & Paulson, J. C. CD22 regulates adaptive and innate immune responses of B cells. *J. Innate Immun.* **3**, 411–419 (2011).
42. Casadevall, A. Antibody-based vaccine strategies against intracellular pathogens. *Curr. Opin. Immunol.* **53**, 74–80 (2018).
43. Hatta, Y. et al. Identification of the gene variations in human *CD22*. *Immunogenetics* **49**, 280–286 (1999).
44. Hunter, C. D. et al. Human neuraminidase isoenzymes show variable activities for 9-*O*-acetyl-sialoside substrates. *ACS Chem. Biol.* **13**, 922–932 (2018).
45. Varki, A., Hooshmand, F., Diaz, S., Varki, N. M. & Hedrick, S. M. Developmental abnormalities in transgenic mice expressing a sialic acid-specific 9-*O*-acetylesterase. *Cell* **65**, 65–74 (1991).
46. Rizzuto, G. et al. Establishment of fetomaternal tolerance through glycan-mediated B cell suppression. *Nature* **603**, 497–502 (2022).
47. Fowler, K. B. et al. The outcome of congenital cytomegalovirus infection in relation to maternal antibody status. *N. Engl. J. Med.* **326**, 663–667 (1992).
48. Boppana, S. B., Rivera, L. B., Fowler, K. B., Mach, M. & Britt, W. J. Intrauterine transmission of cytomegalovirus to infants of women with preconceptional immunity. *N. Engl. J. Med.* **344**, 1366–1371 (2001).
49. Brown, Z. A. et al. Effect of serologic status and cesarean delivery on transmission rates of herpes simplex virus from mother to infant. *JAMA* **289**, 203–209 (2003).
50. Hafner, L. et al. *Listeria monocytogenes* faecal carriage is common and depends on the gut microbiota. *Nat. Commun.* **12**, 6826 (2021).

Methods

Mice

Inbred C57BL/6 mice were purchased from the National Cancer Institute or generated by in-house breeding. *μMT*$^{-/-}$ (002288), *Cd8a*$^{-/-}$ (002665), *Fcer1g*$^{-/-}$ (002847), *Cd22*$^{-/-}$ (006940), *Cd19*$^{cre/cre}$ (*Cd19*$^{-/-}$, 006785), IL-10-eGFP (Vert-X, 014530), *C1q*$^{-/-}$ (031675) and *C3*$^{-/-}$ (029661) mice were purchased from Jackson Laboratories. *St6gal1*$^{-/-}$ mice have been described previously[51]. *Siae*$^{-/-}$ mice were generated by the CCHMC Transgenic Animal and Genome Editing Core by constructing a *Siae*-deficient allele using a dual sgRNA CRISPR–Cas9 method. In brief, three sgRNAs (target sequences: 1, CCTGAGCTTAGCCACAAATG; 2, CATGCAGATGACTGTTTCAC; and 3, GAACCAAATTCAGGGGCTAC) were selected, according to the on- and off-target scores from the web tool CRISPOR (http://crispor.tefor.net)[52] and chemically synthesized by Integrated DNA Technologies. The sgRNA pairs (1 and 2) and (1 and 3) were used to delete exon 3 and exons 3–4 of *Siae*, respectively. To prepare the ribonucleoprotein complex (RNP) for each targeting, we incubated the sgRNA pair (40 ng μl^{-1} per sgRNA) and Cas9 protein (120 ng μl^{-1}; IDT) in Opti-MEM (Thermo Fisher Scientific) at 37 °C for 15 min. The zygotes from superovulated female mice on the C57BL/6J genetic background were electroporated with 7.5 μl RNP on a glass slide electrode using the Genome Editor electroporator (BEX; 30 V, 1 ms width, and 5 pulses with an interval of 1 s). Then 2 min after electroporation, zygotes were moved into 500 μl cold M2 medium (Sigma-Aldrich), warmed up to room temperature and then transferred into the oviductal ampulla of pseudopregnant CD-1 females. Pups were born and genotyped by PCR and Sanger sequencing.

Mice were housed in specific-pathogen free conditions at 25 °C, ambient humidity, a 12 h–12 h day–night cycle, with free access to water and a standard chow diet. Females between 8 and 12 weeks of age were used for all of the experiments. For some experiments, timed mating was performed by synchronized introduction of males to breeding cages. For experiments examining immunodeficient maternal mice, females were mated with WT males to generate heterozygous, immunocompetent offspring. Mice were checked daily for birth timing. Neonatal mice were evaluated from birth (cross-fostering experiments), or between 3–4 days of age as described. Neonates from the same litter were divided among groups for individual experiments. For cross-foster experiments, pups were switched between nursing dams within 12 h of birth. For survival experiments, mice were euthanized when moribund. Adult mice were euthanized by cervical dislocation. Neonates were sacrificed by decapitation. All animal procedures were carried out in accordance with the Institutional Animal Care and Use Committee-approved protocol of Cincinnati Children's Hospital and Medical Center.

Bacteria and infections

Lm (WT strain 10403s or attenuated ΔActA DPL-1942) was grown in brain–heart infusion (BHI) medium at 37 °C, back diluted to early logarithmic phase (optical density at 600 nm of 0.1) and resuspended in sterile PBS as described previously[53,54]. Female mice were preconceptually primed with 10^7 colony-forming units (CFU) of ΔActA*Lm*, injected intravenously. For some experiments, a second injection was given 2–3 weeks later. Mice were mated 5–7 days after priming. For virulent infection, adult mice were inoculated intravenously with a dose of 2×10^4 CFU per mouse, except in the experiment shown in Fig. 1e, in which mice received 10^5 CFU. Neonatal mice were infected with 50–100 CFU intraperitoneally (i.p.). For fungal infections, neonatal mice were infected i.p. with 10^6 CFU of *C. albicans* (strain SC5314) grown in YPAD medium as described previously[55]. The inoculum for each experiment was verified by spreading a diluted aliquot onto agar plates. To assess susceptibility after infection, mouse organs (spleen and liver) were dissected and homogenized in sterile PBS containing 0.05% Triton X-100 to disperse the intracellular bacteria, and serial dilutions of the organ homogenate were spread onto agar plates. Colonies were counted after plate incubation at 37 °C for 24 h.

Serum collection and IgG purification

For phlebotomy, adult mice were bled 200 μl through submandibular bleed or cardiac puncture at the time of euthanasia. For neonates, blood was collected after decapitation. To collect serum, the blood was allowed to clot at room temperature and then centrifuged at 10,000 rpm for 10 min. Serum was removed and then heat inactivated (56 °C for 20 min). Sera were collected separately and pooled from several *Lm*-primed mice. Sera from *Lm*-primed virgin mice (vSera) were collected starting 2 weeks after the last dose of ΔActA *Lm*. Sera from preconceptually *Lm*-primed pregnant mice (pSera) were collected starting from late gestation (around E18) to P7. Adoptive sera transfers were accomplished by i.p. injection in adults (200 μl volume) or neonates (50 μl volume). For breastmilk transfer of antibodies, nursing dams were injected with vSera when the pups were P0 and P3.

Sera containing anti-*Lm* antibodies were purified over protein A columns according to the manufacturer instructions (Abcam, 109209) to obtain the IgG-containing fraction. Purified IgG was concentrated and dialysed to PBS using the Amicon Ultra Pro Purification System (Millipore, ACS510024). Protein G spin columns (Thermo Fisher Scientific, 89953) were used to isolate IgG from individual mice. IgG from naive mice was purified from sera or purchased (Sigma-Aldrich, I5381). Neonates were transferred 50–75 μg purified *Lm*-immune IgG.

ELISA

For evaluating *Lm*-specific antibodies by enzyme-linked immunosorbent assay (ELISA), flat-bottom, high-binding, 96-well enzyme immunoassay/radioimmunoassay plates (Costar) were coated with nearly-confluent log-phase *Lm* 10403S and allowed to dry overnight under ultraviolet light. Alternatively, plates were coated with recombinant LLO toxin at 1 μg ml^{-1} for at least 24 h. Coated plates were then blocked with 3% milk. All of the wash steps were performed in triplicate with PBS + 0.05% Tween-20. Serum from each mouse was diluted 1:10 or 1:20 and then 1:4 serial dilutions were performed followed by staining with the following biotin-conjugated anti-mouse secondary antibodies: rat anti-mouse IgG (eBioscience, 13-4013-8), rat anti-mouse IgM (eBioscience, 13-5890-1589), rat anti-mouse IgA (eBioscience, 13-5994-82), rat anti-mouse IgG1 (BD Pharmingen, 553441), rat anti-mouse IgG2b (BD Pharmingen, 553393), rabbit anti-mouse IgG2c (Invitrogen, SA5-10235) and rat anti-mouse IgG3 (BD Pharmingen, 553401). Each secondary antibody was used at 1:1,000 dilution. Plates were developed with streptavidin peroxidase (BD Bioscience, 554066) using *o*-phenylenediamine dihydrochloride as a substrate and measuring absorbance at 450 nm (A_{450}) as described previously[56]. Antibody titres were quantified as EC_{50} (the point of 50% maximum OD_{450}) using a nonlinear second-order polynomial in Prism (GraphPad).

To detect *N*-glycans, LLO-coated plates were used to avoid staining endogenous glycans present on *Lm* bacteria. Plates were blocked with a carbohydrate-free blocking buffer (VectorLabs, SP-5040-125). Purified IgG was added at 0.1–0.2 mg μl^{-1} final concentration and then biotinylated lectins (from VectorLabs, except where noted) with defined carbohydrate specificity were used as secondary probes: SNA (terminal α2,6-sialic acid, 8 μg ml^{-1}), ECA (β1,4-galactose, 20 μg ml^{-1}), AAL (α1,6-fucose-β1,N-GlcNAc, 20 μg ml^{-1}), UEA (α1,2-fucose, 20 μg ml^{-1}), GSL-II (terminal GlcNAc, 20 μg ml^{-1}), CCA (9-*O*-acetylated and 4-*O*-acetylated sialic acid, EY Labs, BA-7201-1, 10 μg ml^{-1}). Enzymatically deactivated haemagglutinin esterase from mouse hepatitis virus (MHV, 4-*O*-acetylated sialic acid) and porcine torovirus (PToV, 9-*O*-acetylated sialic acid) fused to human IgG1 Fc, and their non-binding mutants, were produced as previously described[57] and used at 1 μg ml^{-1} to probe for acetylated sialic acid variants. Streptavidin peroxidase was then added to bind to biotinylated lectins, while mouse anti-human IgG1-perioxidase (Southern Biotech, 9054-05) was used to detect Fc fusion lectins. Most lectins were detected using *o*-phenylenediamine dihydrochloride as a substrate and A_{450} was measured. For the MHV,

PToV and CCA lectins, the signal was developed using SuperSignal ELISA Femto Maximum Sensitivity Substrate (Thermo Fisher Scientific, 37075) and lumens were measured using the Synergy Neo2 plate reader (BioTek). IL-10 was detected from mouse serum according to the manufacturer's instructions (R&D, DY417) using the SuperSignal ELISA Femto Substrate with an assay dynamic range of 3–1,600 pg ml^{-1}.

LLO-neutralization assay

vIgG or pIgG at various dilutions were preincubated with LLO toxin (2.5 nM in PBS) on ice in a 96-well plate for 15 min before the addition of 4×10^6 sheep erythrocytes (Rockland Labs, R406-0050). Triton X-100 (0.05%) and PBS served as positive and negative controls for haemolysis, respectively. Samples were transferred to a spectrophotometer at 37 °C and the A_{700} was measured at 60 s intervals for 30 min.

SNA lectin fractionation

SNA-agarose (1.5 ml; Vector Labs, AL-1303-2) was added to a column (Bio-Rad, 732-6008). Agarose was washed with 10 ml of buffer (20 mM HEPES, 150 mM NaCl, pH 7.2) and then 1 mg of vIgG diluted to 500 µl total volume was added to the column, which was allowed to drain through by gravity. The flow through plus 5 ml of wash were collected as the unbound fraction. Glycoprotein Eluting Solution (3 ml; Vector-Labs, ES-2100-100) was applied to collect the bound fraction. Both fractions were then concentrated and buffer-exchanged to PBS before downstream analysis.

IgG enzyme treatments

Purified IgG was treated with neuraminidase (NEB, P0720L, 1 µl per 25 µg IgG, pH 5.5) to remove sialic acid and then the enzyme was functionally inactivated by incubation at 55 °C for 10 min. IgG was then separated from neuraminidase by size-exclusion chromatography (100 kDa molecular weight cut-off (MWCO)) before being resialylated using murine ST6Gal1 (Creative Biomart, St6gal1-7036M, 1 µg per 20 µg IgG, pH 7.0) plus 2.5 mM CMP-acetylneuraminic acid (CMP-Neu5Ac, Calbiochem, 5052230001), CMP-glycolylneuraminic acid (CMP-Neu5Gc, Chemily, 98300-80-2) or CMP-9-*O*-acetyl-*N*-acetylneuraminic acid (CMP-9-O-Ac-Neu5Ac) as a substrate. The latter was produced by custom synthesis with structural conformation verified by nuclear magnetic resonance and MS with >95% purity among CMP-sialic acid conjugates based on high-performance liquid chromatography (BOC Sciences, www.bosci.com). As a control, vIgG without neuraminidase pretreatment before ST6Gal1 addition of Neu5Ac was included (referred to as $vIgG^{No\text{-}Neur}$ in Fig. 2). IgG *N*-glycan sialic acid deacetylation was accomplished by treating IgG with SIAE (Creative Biomart, SIAE-15119M, 1 µl per 40 µg IgG, pH 8.0). Glycosylation-modifying enzyme reactions were performed at 37 °C for 20–24 h, except for SIAE-mediated deacetylation, which occurred for 42 h, and success was confirmed by lectin staining. To generate $F(ab')_2$ fragments, IgG was treated with pepsin (Thermo Fisher Scientific, 44988) at pH 4.0, 37 °C for 3 h and purified by protein A and size-exclusion chromatography (50 kDa MWCO) and then buffer-exchanged to PBS. Successful cleavage of Fc was confirmed by MS, lectin blots and ELISA with IgG-subtype-specific secondary antibodies.

SNA lectin blots

IgG or $F(ab')_2$ fragments (2–4 µg) were diluted in Laemmli sample buffer, electrophoresed in 4–20% SDS–PAGE Tris/Glycine gels (BioRad, 4561094) and transferred to PVDF membranes (Millipore, IPVH09120) using a semi-dry blotter (Novex). The membranes were blocked in 100% Superblock/TBS (Thermo Fisher Scientific, 37545) plus 0.05% Tween-20 and then incubated overnight at 4 °C with 2 µg ml^{-1} biotinylated SNA lectin in 10% Superblock/TBS plus 0.05% Tween-20. TBS-T was used to wash the membranes. Neutralite Avidin-HRP (Southern Biotech, 7200-05) was used for detection. Lectin blots were developed using SuperSignal West Pico Plus chemiluminescent substrate (Thermo Fisher Scientific, 34580) and imaged using Image Studio Lite v.5.2 on the LI-COR C-DiGit Blot Scanner.

Lm-specific antibody isolation

Serum from virgin or pregnant mice was buffer-exchanged into 20 mM NaH_2PO_4 pH 7.0, 150 mM NaCl using a HiPrep 26/10 Desalting 53 ml column (Cytiva) and run over a HiTrap Protein G HP 1 ml column (Cytiva) to capture antibodies. Antibodies were eluted with 100 mM glycine ~pH 2 into tubes containing sufficient Tris to neutralize the pH. Ultraviolet light (UV)-inactivated *Lm* (UV Stratalinker 2400, Stratagene, 6 min total treatment) was centrifuged at 4,000 rpm for 5 min to pellet the bacteria. *Lm* pellets were then resuspended in 20 M NaH_2PO_4 pH 7.0, 150 mM NaCl. The pellets were washed by centrifuging for another 5 min, pouring off the supernatant and then resuspending with fresh buffer. Bacteria were washed a total of three times, then the final pellet from 2–8 l of inactivated *Lm* was resuspended with 2.5 ml of virgin- or pregnant-mouse-derived protein-G-purified antibodies at around 0.1–0.2 mg ml^{-1}. This mixture was incubated for 30 min with gentle shaking at room temperature. The bacteria were again centrifuged for 5 min, and the supernatant was discarded. The pellet containing *Lm* and *Lm*-specific antibodies was washed with 10 ml of buffer by resuspension and then then centrifuged for 5 min. The supernatant was discarded before adding 2.5 ml of buffer containing 2 M $MgCl_2$ to elute the *Lm*-specific antibodies from the bacteria. The mixture was incubated with shaking for another 5 min and centrifuged. The supernatant containing *Lm*-specific antibodies was collected and buffer-exchanged using the HiPrep 26/10 Desalting 53 ml column to remove the $MgCl_2$. The antibodies were again purified using a HiTrap Protein G HP 1 ml column, then buffer-exchanged back into 20 mM NaH_2PO_4 pH 7.0, 150 mM NaCl during concentration of the antibodies for downstream applications.

MS analysis

Water (Honeywell), acetonitrile (ACN; Thermo Fisher Scientific) and formic acid (FA; Sigma-Aldrich) were all of LC–MS grade. All other chemicals were of laboratory analytical reagent grade. Samples were reduced, alkylated and then digested into peptides. A solution containing around 20 µg of the protein solution in 50 mM Tris-Cl (pH 7.4) was reduced in a solution of 5 mM dithiothreitol at 45 °C for 45 min, a solution of iodoacetamide was added to bring the solution to 15 mM and then incubated at room temperature in the dark for 45 min. A second aliquot of dithiothreitol was then added to the solution to quench the remaining iodoacetamide. Trypsin or chymotrypsin (Promega, sequencing grade) was added to the solution and allowed to digest for 16 h. The digestion was stopped by briefly heating the solution to 100 °C for 5 min before cooling. The digested material was then injected for LC–MS.

LC–MS/MS was performed on the Orbitrap Eclipse Tribrid MS (Thermo Fisher Scientific) system coupled to an Ultimate RSLCnano 3000 (Thermo Fisher Scientific) and equipped with a nanospray ion source. The prepared samples were injected to the separation column (Acclaim PepMap 100, 75 µm × 15cm). The separation was performed in a linear gradient from low to high acetonitrile containing 0.1% formic acid. Mass spectrometry was carried out in the positive-ion mode where a full MS spectrum was collected at high resolution (120,000) and data dependent MS/MS scans of the highest intensity peaks following higher-energy C-trap dissociation (HCD) fragmentation were collected in the Orbitrap. HCD fragments corresponding to sialic acid oxonium ions were then subsequently fragmented a second time with electron-transfer higher-energy collision dissociation (EThcD) fragmentation. The LC–MS/MS data were analysed using Byonic (v.4.0) software search and glycopeptide annotations were screened manually for b and y ions, glycan oxonium ions and neutral losses. Quantification of peak intensities were calculated manually with the instrument software (Xcalibur, v.4.2) based on deconvoluted spectra. Manual sorting of MS/MS fragmentation to search for oxonium ions consistent with

acetyl-glycolylneuraminic acid (acetyl-Neu5Gc or Neu5Gc,Ac) was also conducted with the instrument software using a 5 ppm range of mass error, which is consistent with MS/MS data collected in the Orbitrap for this instrument.

RNA isolation and qPCR

For mice, spleen RNA was extracted from virgin or pregnant females at late gestation (E18–20). For humans, informed consent was obtained before collection of peripheral blood samples from study volunteers. Samples from pregnant (12–32 weeks of gestation) women were collected through prospective studies investigating pregnancy-associated immunological changes in collaboration with M. A. Elovitz, and samples from non-pregnant volunteers were provided in a deidentified manner through Cincinnati Children's Hospital Translational Core Laboratories Cell Processing core under institutional review board (IRB) approved protocols (University of Pennsylvania IRB protocol 833333; CCHMC IRB protocols 2020-0991). Mononuclear cells were freshly isolated over Ficoll-Hypaque gradients. Frozen buffy coats from non-pregnant and pregnant volunteers were thawed and total RNA was isolated using the RNAaqueous-4PCR kit (Invitrogen, AM1914). cDNA synthesis was performed using the TaqMan Reverse Transcription kit (Applied Biosystems, N808234) with an Oligo-d$(T)_{16}$ nucleotide reverse transcription primer. Quantitative PCR (qPCR) reactions were set up using the Taq Man Fast Advanced Master Mix (Applied Biosystems, 4444556). qPCR was performed on the 7500 Fast Real-Time PCR System (Applied Biosystems) using exon-spanning TaqMan probes (Thermo Fisher Scientific) for mouse *Actb* (Mm04394036_g1), mouse *Siae* (Mm00496036_m1), human *RPL13A* (Hs03043885_g1) or human *SIAE* (Hs00405149_m1). *Siae* gene expression was normalized to the housekeeping gene and the fold increase was calculated using the $2^{-\Delta\Delta C_t}$ method.

In vivo antibody blockade

To block receptors in vivo, mouse pups (aged 3 days) were injected with one of the following purified monoclonal antibodies (BioXcell) or appropriate isotype controls: anti-mouse CD16/CD32 (2.4G2, 100 µg per pup), anti-mouse CD22 (Cy34.1, 100 µg per pup), anti-mouse IL-10R (1B1.3A, 100 µg per pup). Blocking antibodies were given simultaneously with anti-*Lm* antibodies, and neonatal mice were infected with *Lm* the next day.

In vitro B cell stimulation assay

Neonatal spleens from IL-10–eGFP mice were pressed between sterile glass slides to obtain a single-cell suspension, RBCs were lysed, and then cells were filtered over nylon mesh to remove debris. UV-inactivated *Lm* (20 µg ml^{-1} final concentration) or the TLR2 agonist Pam3CSK4 (InvivoGen, 100 ng ml^{-1}) was preincubated with IgG from naive mice, vIgG or pIgG (250 µg ml^{-1}) for 1 h at room temperature. Splenocytes (10^6) were then added to individual wells of a 96-well plate and ultraviolet-inactivated *Lm* + IgG were added. Anti-mouse CD22 (Cy34.1) or mouse IgG1 isotype control was included in some of the wells at 2 µg ml^{-1}. Incubation proceeded at 37 °C for 20 h before analysis of GFP expression using flow cytometry.

Flow cytometry

Fluorophore-conjugated antibodies specific for mouse cell-surface antigens were purchased from BioLegend. The following antibodies were used at 1:200 final dilution: anti-B220 (RA3-6B2, 103211), anti-CD4 (GK1.5, 100409), anti-CD8a (53-6.7, 100709), anti-CD11b (M1/70, 101209), anti-CD11c (N418, 117316), anti-CD45.2 (104, 109821), anti-CD22 (OX-97, 126109/ 126105), anti-CD5 (53-7.3, 100607), anti-IgM (RMM-1, 406513). Single-cell suspension of neonatal splenocytes was first stained with Fixable Viability Dye (eBiosciences, 65-0863-14) and then stained with fluorophore-conjugated antibodies in the presence of Fc block (anti-CD16/32). Data were acquired on the BD FACS Canto system using BD FACS Diva software (v.9) and analysed using FlowJo (v.10).

Quantification and statistical analysis

The number of individual animals used per group is described in each individual figure panel or shown by individual data points that represent the results from individual animals. Statistical tests were performed using Prism (GraphPad) software. Unpaired two-tailed Student's *t*-tests were used to compare differences between two groups. One-way ANOVA with Bonferroni post-test for multiple comparisons was used to evaluate experiments containing more than two groups. Differences in the survival between groups of mice were compared using the log-rank (Mantel–Cox) test. The limit of detection for each assay is denoted by a dotted horizontal line.

Graphics

Graphical depictions including illustrations and the summary model were created using content from BioRender.

Reporting summary

Further information on research design is available in the Nature Research Reporting Summary linked to this paper.

Data availability

All data generated and analysed in this study are included in the Article and the Supplementary Information. The MS proteomics data have been deposited to the ProteomeXchange Consortium through the PRIDE partner repository under dataset identifier PXD033357. Source data are provided with this paper.

51. Hennet, T., Chui, D., Paulson, J. C. & Marth, J. D. Immune regulation by the ST6Gal sialyltransferase. *Proc. Natl Acad. Sci. USA* **95**, 4504–4509 (1998).
52. Haeussler, M. et al. Evaluation of off-target and on-target scoring algorithms and integration into the guide RNA selection tool CRISPOR. *Genome Biol.* **17**, 148 (2016).
53. Way, S. S., Kollmann, T. R., Hajjar, A. M. & Wilson, C. B. Cutting edge: protective cell-mediated immunity to Listeria monocytogenes in the absence of myeloid differentiation factor 88. *J. Immunol.* **171**, 533–537 (2003).
54. Elahi, S. et al. Immunosuppressive CD71$^+$ erythroid cells compromise neonatal host defence against infection. *Nature* **504**, 158–162 (2013).
55. Shao, T. Y. et al. Commensal *Candida albicans* positively calibrates systemic Th17 immunological responses. *Cell Host Microbe* **25**, 404–417 (2019).
56. Turner, L. H. et al. Preconceptual Zika virus asymptomatic infection protects against secondary prenatal infection. *PLoS Pathog.* **13**, e1006684 (2017).
57. Wasik, B. R. et al. Distribution of O-acetylated sialic acids among target host tissues for influenza virus. *mSphere* **2**, e00379-16 (2017).

Acknowledgements We thank F. D. Finkelman for discussions; M. A. Elovitz, C. Lutzko, L. Ray, M. Reynolds, L. Trump-Durbin, and the staff at the CCHMC Translational Core Laboratories Cell Processing core for providing de-identified human peripheral blood samples; and S. Tummala and the staff at CCHMC Research Animal Resources for the care of mice. J.J.E. is supported by NIH grant F32AI145184 and the Child Health Research Career Development Award Program through K12HD028827. S.S.W. is supported by DP1AI131080, R01AI145840, R01AI124657 and U01AI144673, the HHMI Faculty Scholar's Program (grant no. 55108587), the Burroughs Wellcome Fund and the March of Dimes Foundation Ohio Collaborative. A.L.S. is supported by NIH grant T32DK007727. P.A. is supported by R24GM137782 at the Complex Carbohydrate Research Center. The Eclipse mass spectrometer used in the glycan analysis was supported by GlycoMIP, a National Science Foundation Materials Innovation Platform funded through Cooperative Agreement DMR-1933525. A.B.H. is supported by R01GM094363 and R01AI162964. In loving memory of Jane Erickson.

Author contributions J.J.E. and S.S.W. designed the experiments. J.J.E., S.A.-H., A.E.Y., J.L.C.M., T.-Y.S., A.L.S., H.M.-H., Y.W. and G.P. performed the experiments. S.S. provided purified LLO. Y.-C.H. generated SIAE-deficient mice. J.T.Y.L. provided ST6Gal1-deficient mice. B.R.W. and C.R.P. provided PToV lectin. J.J.E., S.A.-H., P.A., A.B.H. and S.S.W. analysed the data. J.J.E. and S.S.W. wrote the manuscript with editorial input from all of the authors.

Competing interests A patent on antibody sialic acid modification has been filed by Cincinnati Children's Hospital, with J.J.E. and S.S.W. listed as inventors (PCT/US2022/018847). A.B.H. has equity in Chelexa BioSciencesand in Hoth Therapeutics, and he serves on the scientific advisory board of Hoth Therapeutics. The other authors declare no competing interests.

Additional information
Supplementary information The online version contains supplementary material available at https://doi.org/10.1038/s41586-022-04816-9.

Correspondence and requests for materials should be addressed to Sing Sing Way.

Peer review information *Nature* thanks Pascal Gangneux, James Paulson and Shiv Pillai for their contribution to the peer review of this work. Peer reviewer reports are available.

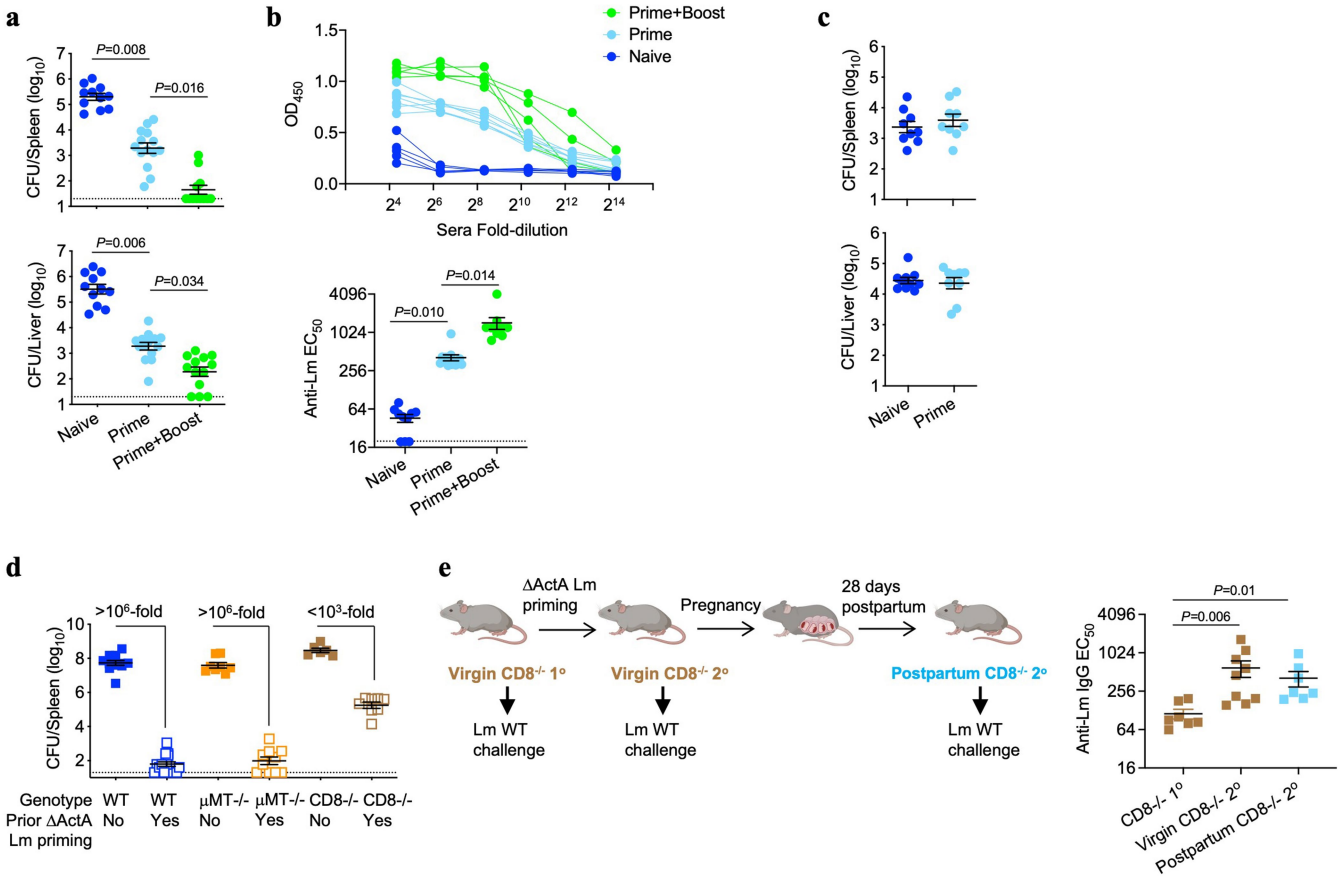

Extended Data Fig. 1 | Pregnancy enables antibody mediated protection against *Lm* infection. (**a**, **b**) Bacterial burden (**a**) and anti-*Lm* IgG titre (**b**) in neonatal mice infected with virulent *Lm* born to WT naive mice or mice preconceptually primed with ΔActA *Lm* once or twice 2 weeks apart. (**c**) *C. albicans* fungal burden in neonatal mice born to WT female mice primed with attenuated ΔActA *Lm* one week prior to mating or naive control mice. Pups were infected with virulent *C. albicans* 3 days after birth, with enumeration of pathogen burden 48 h post-infection. (**d**) Bacterial burden 72 h post-infection with virulent *Lm* in adult WT, μMT-/- or CD8-/- mice with or without ΔActA *Lm* priming 4 weeks prior. (**e**) Anti-*Lm* IgG titre in adult CD8-/- mice 3 days after primary *Lm* infection compared with secondary challenge of ΔActA *Lm*-primed virgin female mice or preconceptually ΔActA *Lm*-primed CD8-/- female mice 3 weeks post-partum. Each symbol represents an individual mouse, with graphs showing data combined from at least 2 independent experiments each with 3-5 mice per group per experiment. Bar, mean ± standard error. *P* values between key groups are shown as determined by one-way ANOVA adjusting for multiple comparisons. Dotted lines, limit of detection.

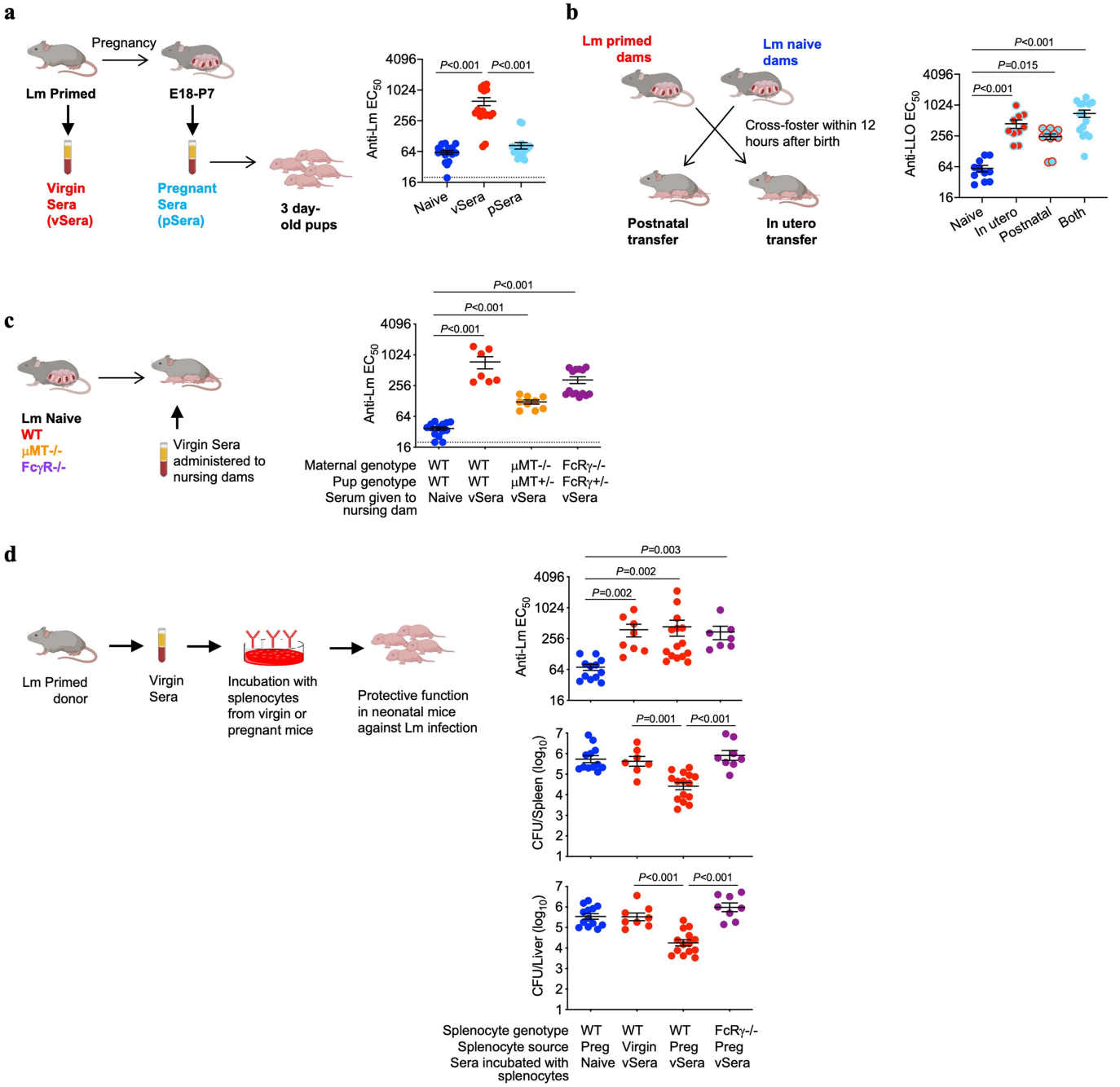

Extended Data Fig. 2 | Anti-*Lm* antibodies acquire protective function during pregnancy through maternal FcγR-expressing cells. (**a**) Anti-*Lm* IgG titre in neonatal mice 72 h after virulent *Lm* infection that were transferred sera from ΔActA *Lm*-primed virgin (vSera) or sera from late gestation/early post-partum (pSera) mice. (**b**) Cross-fostering schematic and anti-*Lm* IgG titre in each group of neonatal mice 72 h after virulent *Lm* infection. (**c**) Anti-*Lm* IgG titre in neonatal mice nursed by WT, µMT-/-, or FcRγ-/- mice administered vSera on the day of delivery and 3 days later. (**d**) Anti-*Lm* IgG titres and bacterial burdens after virulent *Lm* infection in neonatal mice administered vSera that had been incubated with splenocytes from virgin or pregnant (E18) WT or FcRγ-/- mice for 48 h. Pups were infected with virulent *Lm* 3-4 days after birth, 24 h after antibody transfer, with enumeration of bacterial burden 72 h post-infection. Each symbol represents an individual mouse, with graphs showing data combined from at least 2 independent experiments each with 3-5 mice per group per experiment. Bar, mean ± standard error. *P* values between key groups are shown as determined by one-way ANOVA adjusting for multiple comparisons. Dotted lines, limit of detection.

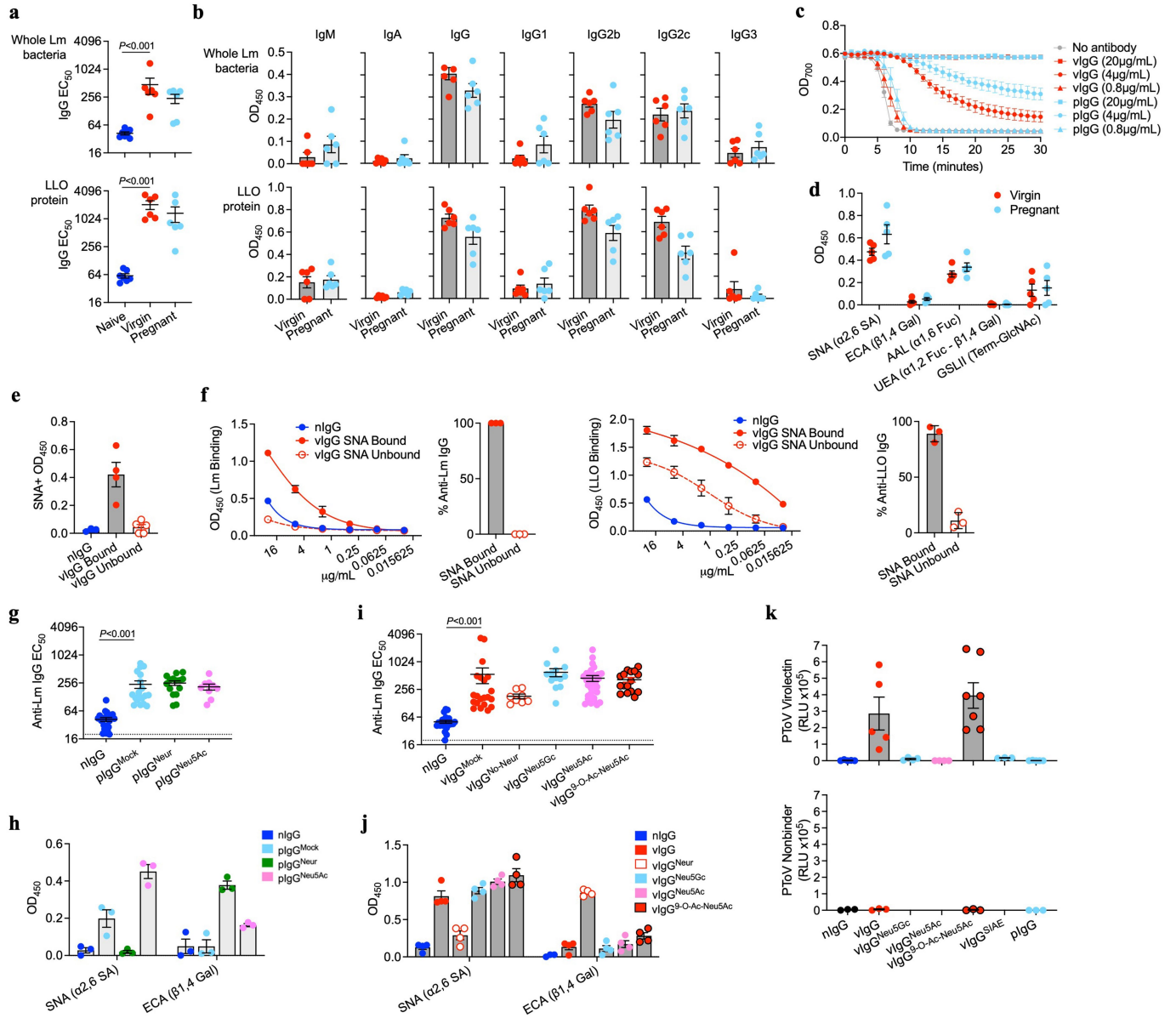

Extended Data Fig. 3 | *Lm*-specific IgG titre, subclass distribution, neutralization efficiency, and lectin staining profile comparisons in virgin compared with pregnant mice. (**a**) IgG titres against UV-inactivated *Lm* bacteria or purified LLO protein for WT female pregnant/postpartum mice preconceptually primed with ΔActA *Lm*, ΔActA *Lm*-primed virgin mice, or naive control mice. (**b**) OD_{450} for each antibody isotype or subclass in sera from ΔActA *Lm*-primed virgin or pregnant mice. All sera diluted 1:100. Background subtracted from staining using naive sera. (**c**) LLO-induced haemolysis of sheep erythrocytes in media containing anti-*Lm* IgG from virgin (vIgG) or late gestation/early postpartum pregnant (pIgG) mice. (**d**) Relative vIgG and pIgG binding to each lectin with defined carbohydrate-specificity for LLO-specific IgG. (**e**,**f**) SNA-agarose fractionation of sialylated (SNA Bound) compared with non-sialylated (SNA Unbound) anti-*Lm* vIgG. SNA lectin staining confirmed successful separation (**e**). *Lm*- and LLO-specific IgG was titred from each fraction (**f**). (**g**, **h**) Anti-*Lm* IgG titre in neonatal mice transferred each type of enzymatically-treated pIgG (**g**). Lectin staining to confirm de- and resialylation of pIgG: SNA signal indicates presence of terminal sialic acid and ECA signal indicates presence of galactose uncovered by terminal sialic acid removal (**h**). (**i**–**k**) Anti-*Lm* IgG titre in neonatal mice transferred glycoengineered vIgG (**i**). SNA and ECA Lectin staining to confirm de- and resialylatoin of vIgG with sialic acid variants (**j**). PToV virolectin probe for 9-O-acetylated sialic acid and PToV with mutated binding site (nonbinder) demonstrating specificity for vIgG resialylated with each sialic acid variant or deacetylated with SIAE treatment (**k**). Representative data from at least 2-3 independent experiments (**a**–**f**) or combined data from 3 independent experiments with 3-5 mice per group per experiment (**g**–**k**) are shown. Bar, mean ± standard error. *P* values between key groups are shown as determined by one-way ANOVA adjusting for multiple comparisons. Dotted lines, limit of detection.

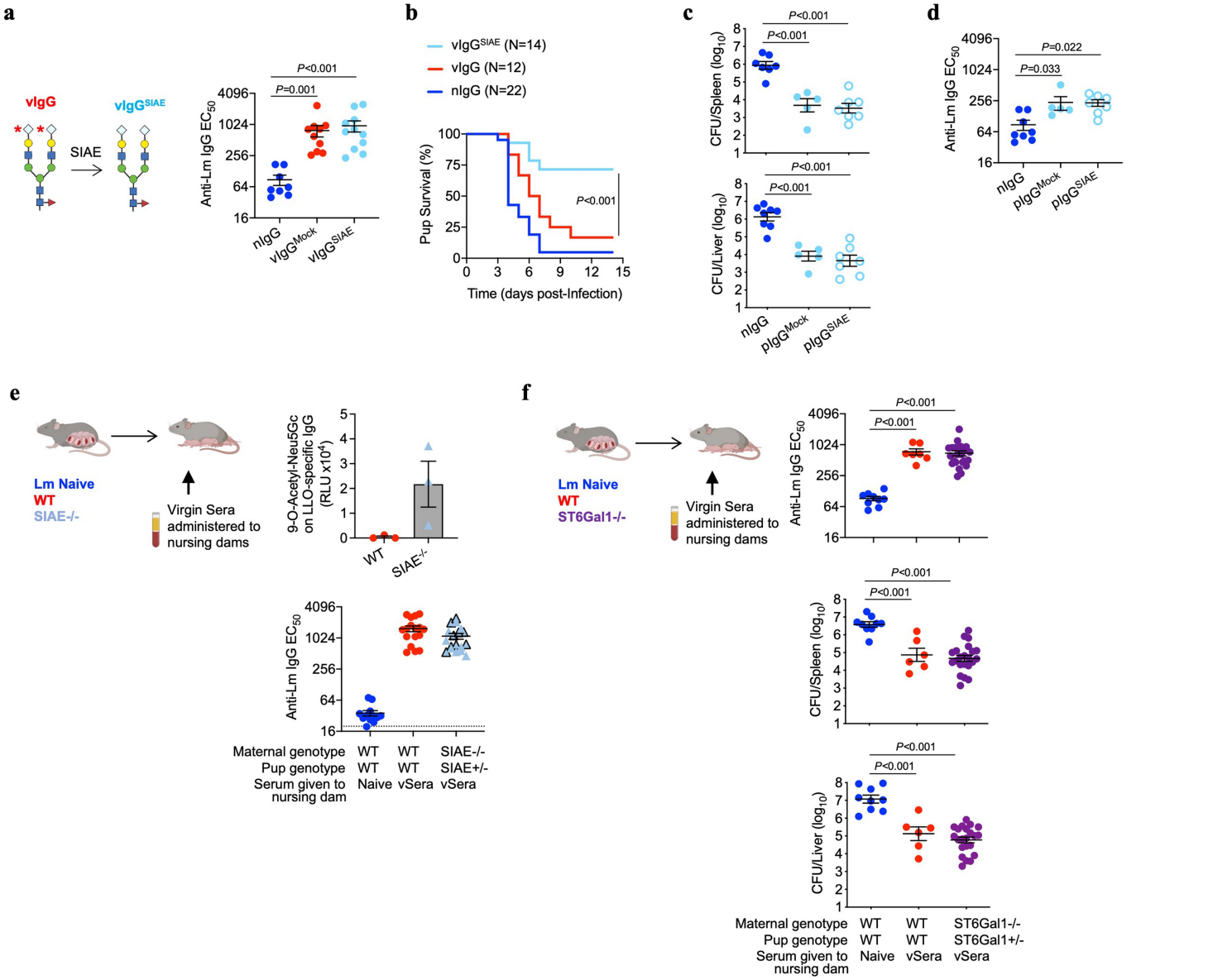

Extended Data Fig. 4 | Deacetylated sialic acid on *Lm*-specific IgG enables antibody-mediated protection. (**a**, **b**) Anti-*Lm* IgG titre 72 h post-infection (**a**) and survival in neonatal mice transferred SIAE- or mock-treated anti-*Lm* IgG from ΔActA *Lm*-primed virgin mice (**b**). (**c**, **d**) Bacterial burden (**c**) and anti-*Lm* IgG titre in neonatal mice infected with virulent *Lm* transferred SIAE- or mock-treated anti-*Lm* IgG from preconceptual ΔActA *Lm*-primed late gestation/early postpartum mice (**d**). (**e**) CCA lectin detection of 9-O-Acetyl-Neu5Gc on LLO-specific IgG obtained 72 h after transferring sera from virgin ΔActA *Lm*-primed mice (vSera) to WT or SIAE KO postpartum recipients on the day of delivery and 3 days later (top). Anti-*Lm* IgG titre in neonatal mice nursed by these females 72 h post-infection with virulent *Lm* (bottom). (**f**) Anti-*Lm* IgG titres (top) and bacterial burdens (bottom) in virulent *Lm* infected neonatal mice nursed by WT or ST6Gal1 KO mice administered vSera as described in panel (**e**). Pups were infected with virulent *Lm* 3-4 days after birth, 24 h after antibody transfer, with enumeration of bacterial burden 72 h post-infection. Each symbol represents an individual mouse, with graphs showing data combined from at least 2 independent experiments each with 3-5 mice per group per experiment. Bar, mean ± standard error. *P* values between key groups are shown as determined by one-way ANOVA adjusting for multiple comparisons (**a**, **c**, **d**, **f**), or Log-rank (Mantel-Cox) test (**b**). Dotted lines, limit of detection.

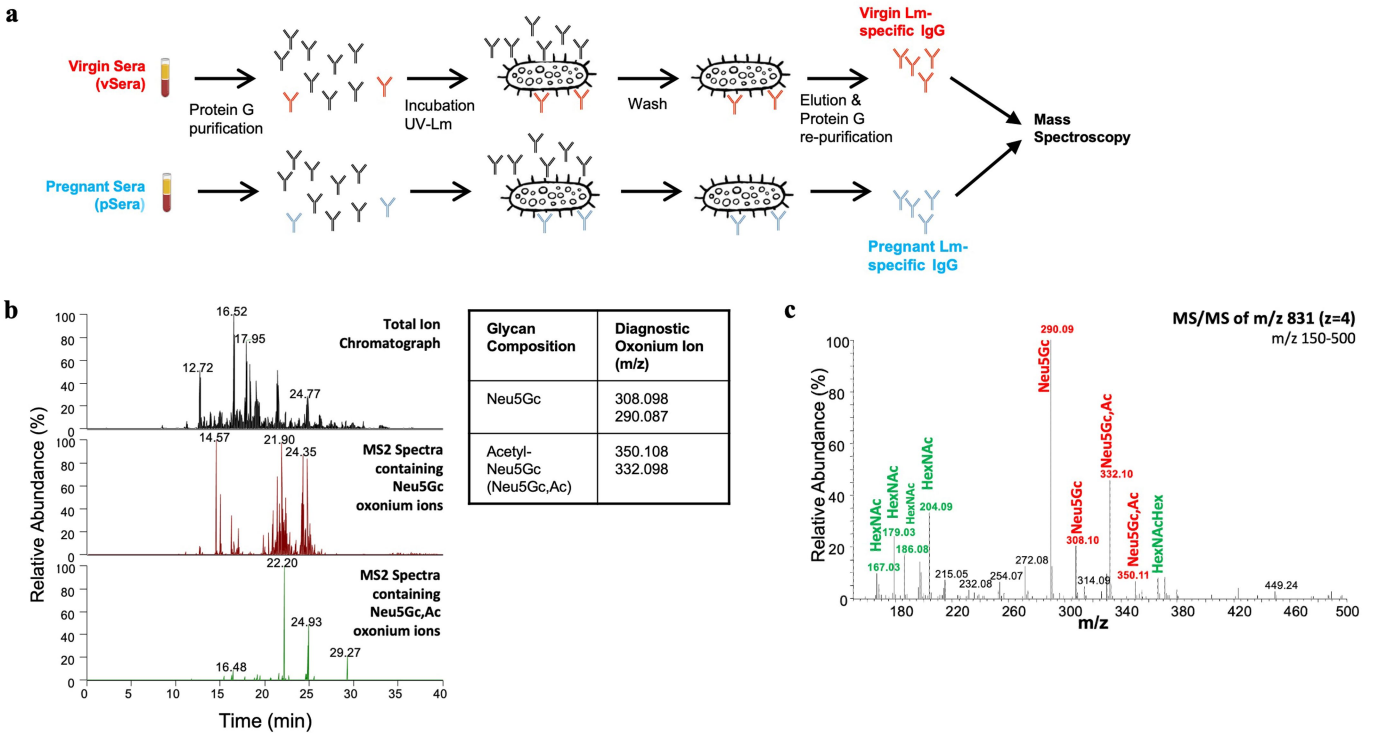

Glycan Composition	Diagnostic Oxonium Ion (m/z)
Neu5Gc	308.098 290.087
Acetyl-Neu5Gc (Neu5Gc,Ac)	350.108 332.098

Extended Data Fig. 5 | Oxonium ion searches for sialic acid modifications. (**a**) Schematic for purification of *Lm*-specific IgG from ΔActA *Lm*-primed virgin and pregnant mice for mass spectroscopy analysis. (**b**) Oxonium ion m/z used to search for sialic acid variants. Diagnostic ions were filtered through the MS/MS spectra to select glycopeptides containing Acetyl-Neu5Gc (Neu5Gc,Ac). Example spectra shown for virgin *Lm*-specific IgG. (**c**) MS/MS fragmentation for the low mass region (150-500) demonstrating sialic acid variants. All presented m/z are z = 1. Experiment was performed in triplicate with representative data shown.

a

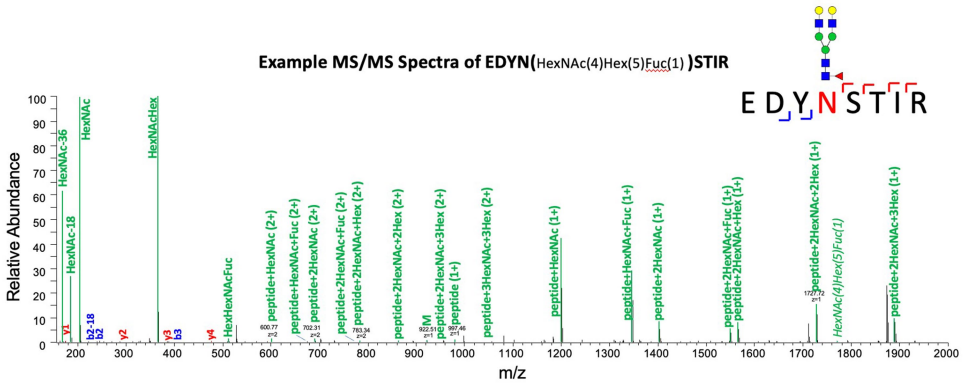

b

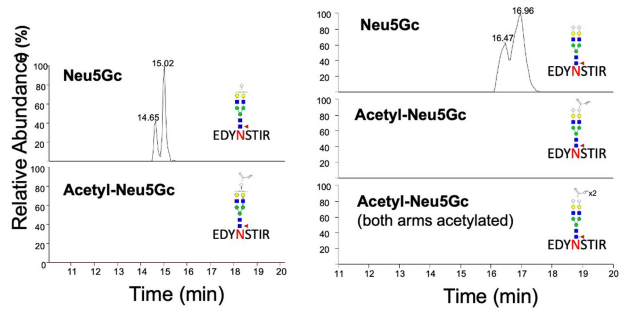

c **Glycoforms observed on the conserved IgG2b N-glycosylation site (peptide EDYNSTIR) for Virgin Lm-specific IgG**

Sequence	Obs. MH	ppm err.	Scan rime	Glycan composition	Proposed glycoform	Average (N=3; ±SD)
R.EDYN[+1444.53387]STIR.V	2441.99	-1.13	13.92	HexNAc(4)Hex(3)Fuc(1)		13 ± 1%
R.EDYN[+1606.58669]STIR.V	2604.041	-1.59	13.97	HexNAc(4)Hex(4)Fuc(1)		44 ± 4%
R.EDYN[+1768.63952]STIR.V	2766.095	-1.2	13.38	HexNAc(4)Hex(5)Fuc(1)		16 ± 1%
R.EDYN[+2075.72985]STIR.V	3073.186	-0.94	14.57	HexNAc(4)Hex(5)Fuc(1) NeuGc(1)		20 ± 3%
R.EDYN[+2237.78267]STIR.V	3235.238	-0.92	14.58	HexNAc(4)Hex(6)Fuc(1) NeuGc(1)		2 ± 1%
R.EDYN[+2382.82018]STIR.V	3380.276	-0.78	16.33	HexNAc(4)Hex(5)Fuc(1) NeuGc(2)		3 ± 1%

d **Glycoforms observed on the conserved IgG2b N-glycosylation site (peptide EDYNSTIR) for Pregnant Lm-specific IgG**

Sequence	Obs. MH	ppm err.	Scan time	Glycan composition	Proposed glycoform	Average (N=3; ±SD)
R.EDYN[+1403.50732]STLR.V	2400.962	-1.48	13.62	HexNAc(3)Hex(4)Fuc(1)		2 ± 1%
R.EDYN[+1444.53387]STLR.V	2441.99	-0.98	13.51	HexNAc(4)Hex(3)Fuc(1)		16 ± 1%
R.EDYN[+1606.58669]STLR.V	2604.043	-1.03	14.2	HexNAc(4)Hex(4)Fuc(1)		61 ± 4%
R.EDYN[+2075.72985]STLR.V	3073.183	-1.89	16	HexNAc(4)Hex(5)Fuc(1) NeuGc(1)		19 ±3%
R.EDYN[+2382.82018]STLR.V	3380.274	-1.54	16.65	HexNAc(4)Hex(5)Fuc(1) NeuGc(2)		3 ±2%

Extended Data Fig. 6 | Glycoforms on IgG2 Fc conserved region N-glycans do not contain acetylated sialic acid. *Lm*-specific IgG from ΔActA *Lm*-primed virgin and pregnant mice was subjected to trypsin or chymotrypsin digestion and then LC-MS/MS analysis. (**a**) Representative MS/MS fragmentation from the conserved N-linked glycosylation site at position 183 on the Fc region of IgG2b/c (glycopeptide EDY**N**STIR). (**b**) Extracted ion chromatograph of EDY**N**STIR with the observed sialic acid (Neu5Gc) glycoforms and the absence of Acetyl-Neu5Gc, which was confirmed for the entire length of the LC-MS run. (**c**, **d**) All glycoforms with observed masses for N-glycans on the conserved Fc region of IgG2b/c for virgin (**c**) and pregnant (**d**) *Lm*-specific IgG. Experiment was performed in triplicate with representative (**a**, **b**) and combined (**c**, **d**) data shown.

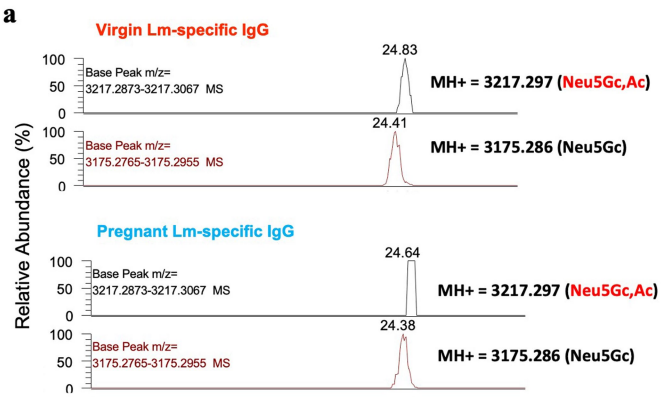

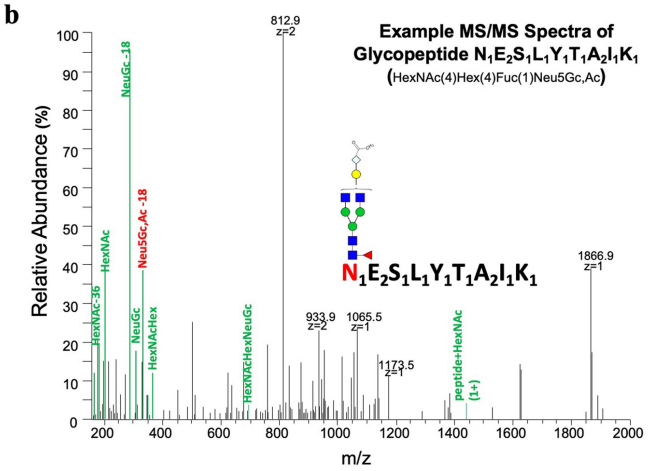

c

Amino acid composition and N-linked glycoforms for novel Fab region peptides containing Acetyl-Neu5Gc.

Sequence	Obs. MH	ppm err.	Glycan composition	Proposed glycoform
$N_1E_2S_1L_1Y_1T_1A_2I_1K_1$	3195.3065	0.41	HexNAc(4)Hex(4)Fuc(1) Neu5Gc,Ac(1)	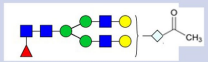
$A_1N_1G_2T_3P_1I_1Q_1V_1D_1S_1$	3217.2971	-0.13	HexNAc(4)Hex(4)Fuc(1) Neu5Gc,Ac(1)	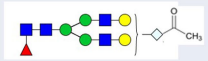

Extended Data Fig. 7 | Acetylated sialic acid localizes to the IgG Fab variable region. (**a**) Extracted ion chromatograph showing m/z corresponding to Acetyl-Neu5Gc (Neu5Gc,Ac) and m/z of the same glycopeptides containing Neu5Gc. Examples of two individual glycopeptides are shown. (**b**) Representative MS/MS fragmentation of glycopeptide $N_1E_2S_1L_1Y_1T_1A_2I_1K_1$ demonstrating presence of Acetyl-Neu5Gc (Neu5Gc,Ac). (**c**) For Fab glycans, the exact amino acid position and sequence are unknown, and shown are potential amino acid compositions given the observed mass size. Experiment was performed in triplicate with representative (**a**, **b**) and combined (**c**) data shown.

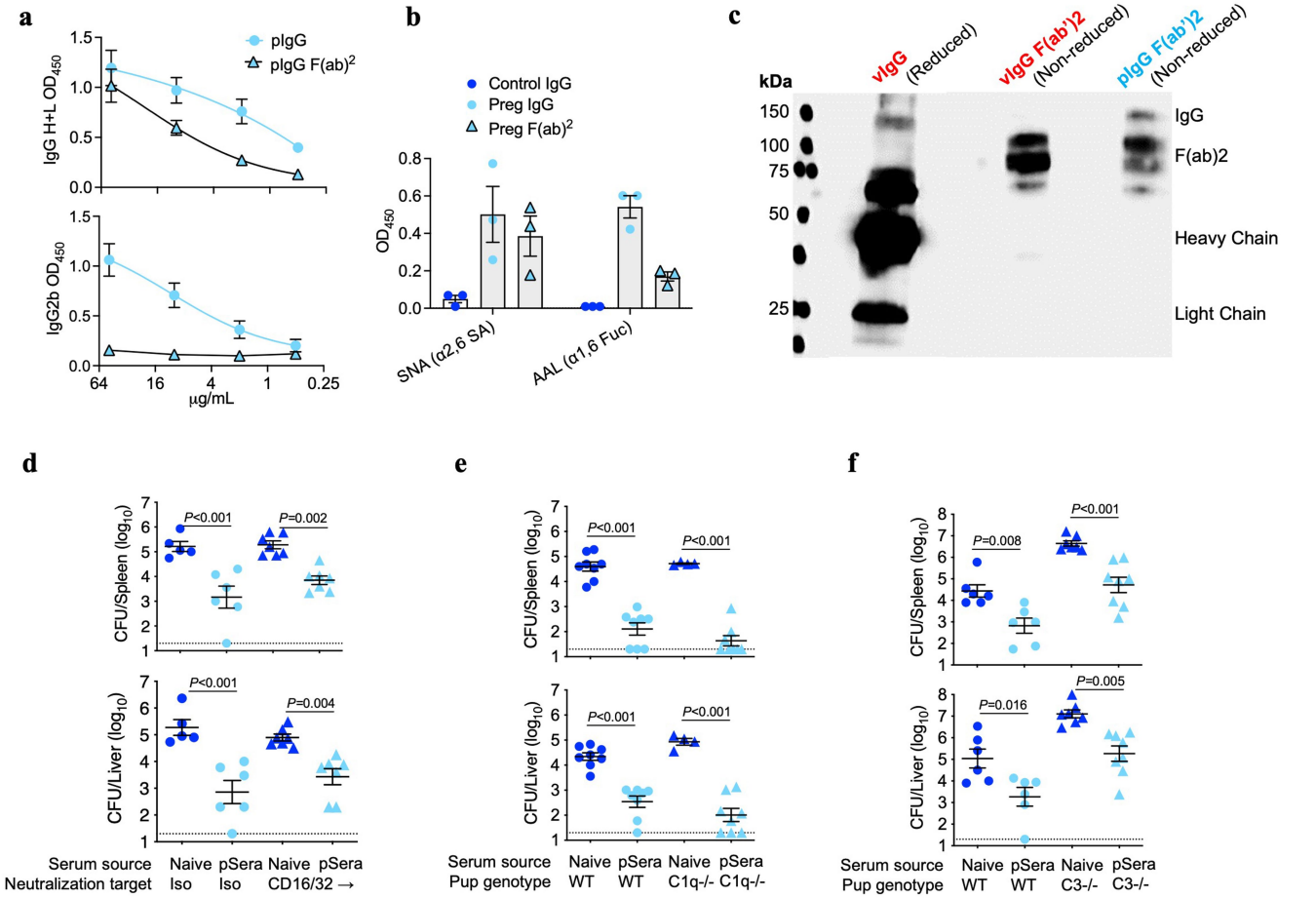

Extended Data Fig. 8 | Fc-mediated functions are dispensable for antibody-mediated protection against *Lm*. (**a**) Presence of IgG heavy (H) and light (L) chains or IgG2b Fc for pF(ab')$_2$ confirming efficient Fc removal after pepsin digestion. (**b**) Lectin staining for pF(ab')$_2$ compared with full-length pIgG for anti-LLO antibodies showing Fab glycosylation. SNA binds α2,6-linked sialic acid residues, while AAL binds α1,6-linked fucose. (**c**) SNA lectin blot comparing full-length IgG under reducing conditions to separate heavy and light chains, with purified F(ab')$_2$ fragments under non-reducing conditions, demonstrating preserved SNA lectin staining. (**d**) Bacterial burden after virulent *Lm* infection in neonatal mice transferred sera from preconceptual ΔActA *Lm*-primed pregnant/postpartum (pSera) or naive control mice, along with anti-CD16/32 blocking or isotype control antibodies. (**e**, **f**) Bacterial burden after virulent *Lm* infection in neonatal WT, complement C1q-deficient mice (**e**) or complement C3-deficient (**f**) transferred pSera or sera from naive mice. Pups were infected with virulent *Lm* 3-4 days after birth, 24 h after antibody transfer, with enumeration of bacterial burden 72 h post-infection. Each symbol represents an individual mouse, with graphs showing data combined from at least 2 independent experiments each with 3-5 mice per group per experiment. Gel is representative of results from 3 independent experiments each with similar results (**c**). Bar, mean ± standard error. *P* values between key groups are shown as determined by one-way ANOVA adjusting for multiple comparisons. Dotted lines, limit of detection.

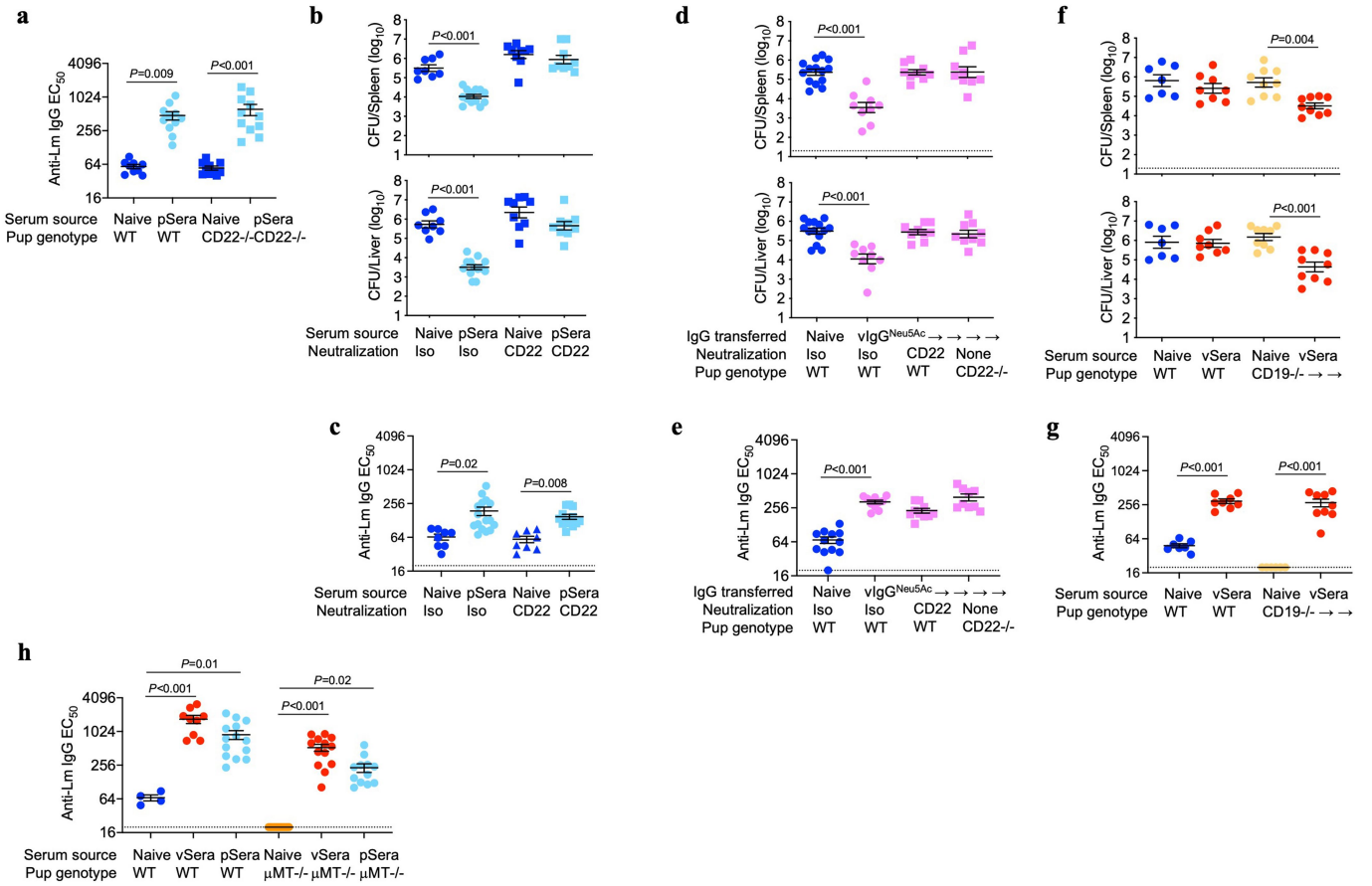

Extended Data Fig. 9 | Deacetylated anti-*Lm* antibodies protect via CD22-mediated suppression of B cell IL-10 production. (**a**) Anti-*Lm* antibody titres in neonatal WT or CD22-deficient mice transferred sera from ΔActA *Lm*-primed pregnant/postpartum (pSera) or naive mice. (**b**, **c**) Bacterial burden (**b**) or anti-*Lm* IgG titres (**c**) after virulent *Lm* infection in neonatal mice transferred pSera or sera from naive mice along with anti-CD22 blocking or isotype control antibodies. (**d**, **e**) Bacterial burden (**d**) or anti-*Lm* IgG titres (**e**) after virulent *Lm* infection in neonatal mice transferred vIgG glycoengineered to express Neu5Ac. Neonates received either isotype control mAb or anti-CD22 mAb, or were CD22 deficient. (**f**, **g**) Bacterial burden (**f**) and anti-*Lm* IgG titres (**g**) after virulent *Lm* infection in WT or CD19-/- neonatal mice transferred vSera or sera from naive mice. (**h**) Anti-*Lm* IgG titres in neonatal WT or µMT-/- mice transferred sera from ΔActA *Lm*-primed virgin (vSera) or pSera. Each symbol represents an individual mouse, with graphs showing data combined from at least 2 independent experiments each with 3-5 mice per group per experiment. Bar, mean ± standard error. *P* values between key groups are shown as determined by one-way ANOVA adjusting for multiple comparisons. Dotted lines, limit of detection.

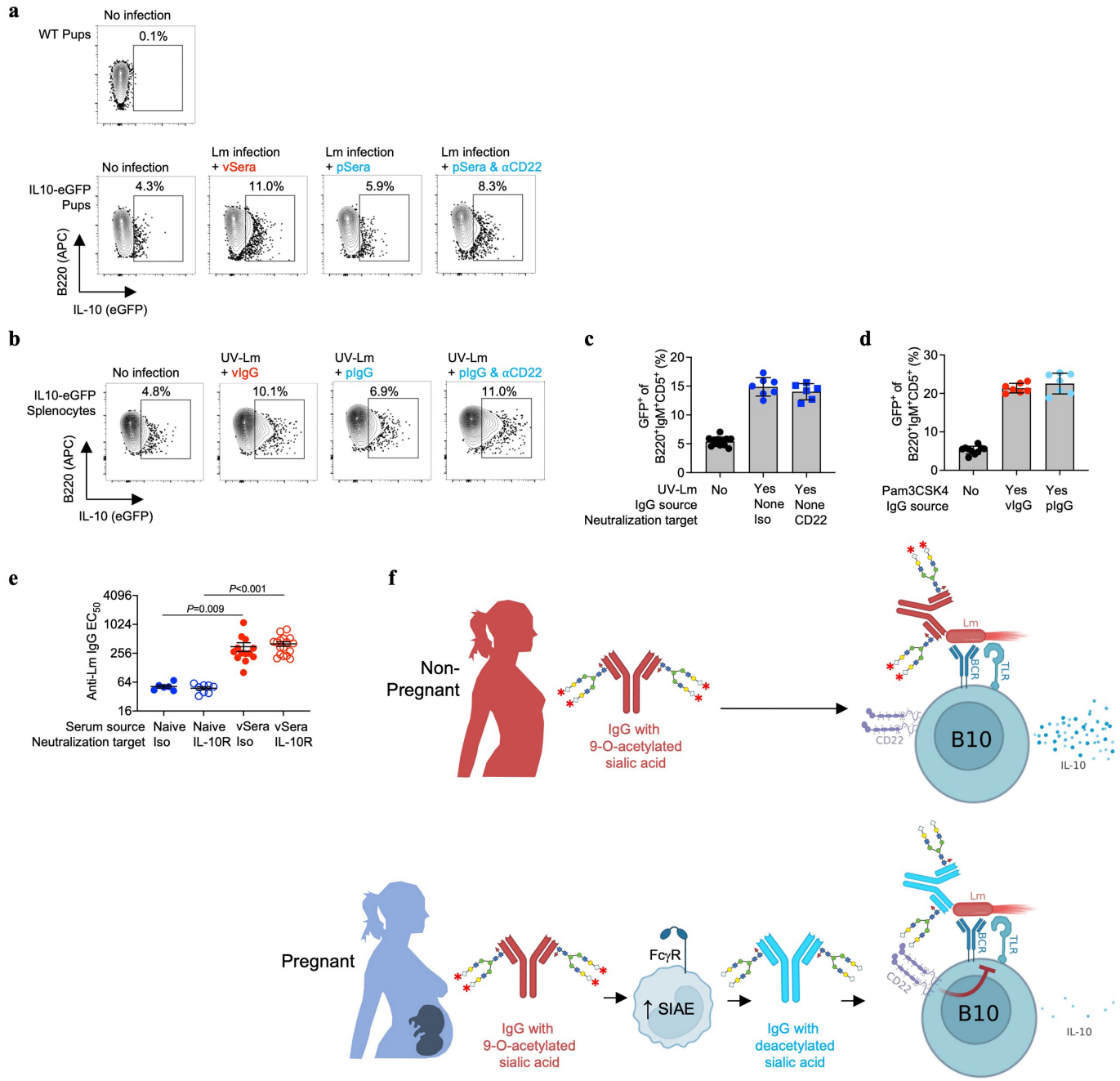

Extended Data Fig. 10 | Deacetylated anti-*Lm* antibodies protect via CD22-mediated suppression of B cell IL-10 production. (**a**) Representative FACS plots showing GFP expression by B220$^+$IgM$^+$CD5$^+$ splenocytes 72 h after virulent *Lm* infection in neonatal IL10-eGFP reporter mice administered vSera or pSera along with anti-CD22 neutralizing or isotype control antibodies, compared with no infection control mice. (**b**) Representative FACS plots showing GFP expression by B220$^+$IgM$^+$CD5$^+$ splenocytes from IL10-eGFP reporter mice stimulated with UV-inactivated *Lm* for 20 h in the presence of vIgG or pIgG plus anti-CD22 neutralizing antibody or isotype control. (**c**) GFP expression by B220$^+$IgM$^+$CD5$^+$ splenocytes from IL10-eGFP reporter mice after UV-*Lm* stimulation plus anti-CD22 neutralizing antibody or isotype control without anti-*Lm* IgG. (**d**) GFP expression by B220$^+$IgM$^+$CD5$^+$ splenocytes from IL10-eGFP reporter mice stimulated with the TLR2 agonist Pam3CSK4 in the presence of vIgG or pIgG. (**e**) Anti-*Lm* antibody titres in neonatal mice transferred vSera or sera from naive mice along with anti-IL10 receptor blocking or isotype control antibodies. (**f**) Model of pregnancy-induced deacetylation of anti-*Lm* antibodies that unleash their protective function by overriding IL-10 production by B10 cells via CD22. Each symbol represents the data from cells in an individual well under unique stimulation conditions combined from 4-5 independent experiments (**c**, **d**), or individual mice (**e**) with graphs showing data combined from at least 2 independent experiments with 3-5 mice per group per experiment. Bar, mean ± standard error. *P* values between key groups are shown as determined by one-way ANOVA adjusting for multiple comparisons.

nature portfolio

Corresponding author(s): Sing Sing Way

Last updated by author(s): Apr 8, 2022

Reporting Summary

Nature Portfolio wishes to improve the reproducibility of the work that we publish. This form provides structure for consistency and transparency in reporting. For further information on Nature Portfolio policies, see our Editorial Policies and the Editorial Policy Checklist.

Statistics

For all statistical analyses, confirm that the following items are present in the figure legend, table legend, main text, or Methods section.

n/a	Confirmed	
☐	☒	The exact sample size (*n*) for each experimental group/condition, given as a discrete number and unit of measurement
☐	☒	A statement on whether measurements were taken from distinct samples or whether the same sample was measured repeatedly
☐	☒	The statistical test(s) used AND whether they are one- or two-sided *Only common tests should be described solely by name; describe more complex techniques in the Methods section.*
☐	☒	A description of all covariates tested
☐	☒	A description of any assumptions or corrections, such as tests of normality and adjustment for multiple comparisons
☐	☒	A full description of the statistical parameters including central tendency (e.g. means) or other basic estimates (e.g. regression coefficient) AND variation (e.g. standard deviation) or associated estimates of uncertainty (e.g. confidence intervals)
☐	☒	For null hypothesis testing, the test statistic (e.g. *F*, *t*, *r*) with confidence intervals, effect sizes, degrees of freedom and *P* value noted *Give P values as exact values whenever suitable.*
☒	☐	For Bayesian analysis, information on the choice of priors and Markov chain Monte Carlo settings
☒	☐	For hierarchical and complex designs, identification of the appropriate level for tests and full reporting of outcomes
☒	☐	Estimates of effect sizes (e.g. Cohen's *d*, Pearson's *r*), indicating how they were calculated

Our web collection on statistics for biologists contains articles on many of the points above.

Software and code

Policy information about availability of computer code

Data collection	Flow cytometry: Data was collected by BD FACS Diva software (ver 9 for Windows)
Data analysis	Flow cytometry: Flowjo (ver 10 for MacOS) Statistical analysis: Prism GraphPad (ver 9 for MacOS) Mass spectroscopy: Byonic (ver 4)

For manuscripts utilizing custom algorithms or software that are central to the research but not yet described in published literature, software must be made available to editors and reviewers. We strongly encourage code deposition in a community repository (e.g. GitHub). See the Nature Portfolio guidelines for submitting code & software for further information.

Data

Policy information about availability of data

All manuscripts must include a data availability statement. This statement should provide the following information, where applicable:

- Accession codes, unique identifiers, or web links for publicly available datasets
- A description of any restrictions on data availability
- For clinical datasets or third party data, please ensure that the statement adheres to our policy

The datasets generated and/or analyzed in the current study are available from the corresponding author on reasonable request.

Field-specific reporting

Please select the one below that is the best fit for your research. If you are not sure, read the appropriate sections before making your selection.

☒ Life sciences ☐ Behavioural & social sciences ☐ Ecological, evolutionary & environmental sciences

For a reference copy of the document with all sections, see nature.com/documents/nr-reporting-summary-flat.pdf

Life sciences study design

All studies must disclose on these points even when the disclosure is negative.

Sample size	For mouse studies, we generally start experiments with 10 mice per group with 90% statistical power to detect a 50% difference in response. Pilot experiments are performed under these assumptions, with sample size adjusted accordingly. For biochemical and mass spectroscopy studies, the sample size in each experiment were based on feasibility and results of prior experiments. To ensure reproducibility, each experiment was replicated using independent samples obtained from separate groups of mice, with statistical analysis performed on pooled data.
Data exclusions	In general, no data are excluded, with the possible exception that the inoculum for each infection experiment was verified by plating and if the dosage was off by >50% of expected, the entire experiment was excluded.
Replication	All experiments were performed at least two times, often with 3-4 separate experiments, each with similar results to confirm the reproducibility of results. For data showing negative results, at least 2 independent experiments were performed.
Randomization	All pups in each litter were randomly assigned to either specific experimental or control groups, with equal distribution of mice in each group. Randomization was not possible for in vitro experiments where the identity of each antibody type/source was already known.
Blinding	Assays of antibody titer and plating of pathogen burden were performed in a blinded fashion. Otherwise, our experiments did not include any subjective scoring or analysis that would require blinding. A large fraction of the data were bacterial burdens and antibody titers which are parameters that are completely observer independent and not subject to investigator bias.

Reporting for specific materials, systems and methods

We require information from authors about some types of materials, experimental systems and methods used in many studies. Here, indicate whether each material, system or method listed is relevant to your study. If you are not sure if a list item applies to your research, read the appropriate section before selecting a response.

Materials & experimental systems

n/a	Involved in the study
☐	☒ Antibodies
☒	☐ Eukaryotic cell lines
☒	☐ Palaeontology and archaeology
☐	☒ Animals and other organisms
☐	☒ Human research participants
☒	☐ Clinical data
☒	☐ Dual use research of concern

Methods

n/a	Involved in the study
☒	☐ ChIP-seq
☐	☒ Flow cytometry
☒	☐ MRI-based neuroimaging

Antibodies

Antibodies used	ELISA: Serum from each mouse was diluted 1:10 or 1:20 and then 1:4 serial dilutions were performed followed by staining with the following biotin-conjugated anti-mouse secondary antibodies: rat anti-mouse IgG (eBioscience, 13-4013-8), rat anti-mouse IgM (eBioscience, 13-5890-1589), rat anti-mouse IgA (eBioscience, 13-5994-82), rat anti-mouse IgG1 (BD Pharmingen, cat. no. 553441), rat anti-mouse IgG2b (BD Pharmingen, 553393), rabbit anti-mouse IgG2c (Invitrogen, SA5-10235), and rat anti-mouse IgG3 (BD Pharmingen, 553401). Each secondary antibody was used at 1:1,000 dilution. Mouse anti-human IgG1-perioxidase (Southern Biotech, 9054-05) was used to detect Fc fusion virolectins. Flow Cytometry: The following antibodies from BioLegend (clone, cat #,) were used at 1:200 final dilution: anti-B220 (RA3-6B2, 103211), anti-CD4 (GK1.5, 100409), anti-CD8a (53-6.7, 100709), anti-CD11b (M1/70, 101209), anti-CD11c (N418, 117316), anti-CD45.2 (104, 109821), anti-CD22 (OX-97, 126109/ 126105), anti-CD5 (53-7.3, 100607), anti-IgM (RMM-1, 406513). In vivo blockade: To block receptors in vivo, 3-day old mouse pups were injected with one of the following purified monoclonal antibodies (BioXcell) or appropriate isotype controls: anti-mouse CD16/CD32 (2.4G2, 100µg/pup), anti-mouse CD22 (Cy34.1, 100µg/pup), anti-mouse IL-10R (1B1.3A, 100µg/pup).
Validation	Antibodies are all from established commercial vendors that perform rigorous species-specific QC testing for each lot. Specific

Validation	statements of validation include: BioLegend: "Specificity testing of 1-3 target cell types with either single- or multi-color analysis (including positive and negative cell types). Once specificity is confirmed, each new lot must perform with similar intensity to the in-date reference lot. Brightness (MFI) is evaluated from both positive and negative populations. Each lot product is validated by QC testing with a series of titration dilutions." Invitrogen (ThermoFisher) "Antibodies are currently undergoing a rigorous 2-part testing approach; Part 1 = Target specificity verification, Part 2 = Functional application validation." BioXcell: "...the InVivoMAb and InVivoPlus versions of the same clone are the exact same antibody with the same functional properties, applications, and formulation. The difference is in the quality control (QC) included. The InVivoPlus version is validated for antigen binding, screened for murine pathogens, and screened for aggregates while the InVivoMAb version is not. Both the InVivoMAb and InVivoPlus formats are perfectly suited for in vivo use..."

Animals and other organisms

Policy information about studies involving animals; ARRIVE guidelines recommended for reporting animal research

Laboratory animals	Mice were housed in specific pathogen-free conditions at 25 degrees Celsius, ambient humidity, a 12 hour day/night cycle, with free access to water and a standard chow diet. Experiments employed pregnant and non-pregnant female mice at 8-12 weeks of age. Neonatal mice were evaluated from birth (cross-fostering experiments), or between 3-4 days of age as described in the manuscript methods. Inbred C57BL/6 mice were purchased from the National Cancer Institute or generated by in-house breeding. uMT-/- (002288), CD8-/- (002665), FcR gamma chain-/- (002847), CD22-/- (006940), CD19Cre/Cre (CD19-/-, 006785), IL10-eGFP (Vert-X, 014530), C1q-/- (031675) and C3-/- (029661) were purchased from Jackson Laboratories (stock number). ST6Gal1-/- mice were a gift from Joseph Lau (Roswell Park, Rochester, NY). SIAE-/- mice were generated by the CCHMC Transgenic Animal and Genome Editing Core.
Wild animals	The study did not involve wild animals.
Field-collected samples	The study did not involve samples collected from the field.
Ethics oversight	All experiments involving animals were performed under Cincinnati Children's Hospital institution Animal Care and Use Committee approved protocol

Note that full information on the approval of the study protocol must also be provided in the manuscript.

Human research participants

Policy information about studies involving human research participants

Population characteristics	Given the focus on pregnancy, the population was limited to female sex and reproductive age (18-45 years)
Recruitment	Pregnant women were recruited from OB/GYN clinics at the time of regularly scheduled prenatal visits. They were screened by study staff for eligibility based on objective inclusion criteria without bias and informed consent was obtained prior to specimen collection. Peripheral blood from pregnant (12-32 weeks of gestation) women were collected through prospective studies investigating pregnancy associated immunological changes in collaboration with Dr. Michal A. Elovitz (University of Pennsylvania), and specimens from non-pregnant volunteers recruited without bias provided in a de-identified fashion through Cincinnati Children's Hospital Translational Core Laboratories Cell Processing core.
Ethics oversight	The collection, use and analysis of human specimens were approved through institutional review board (IRB) approved protocols (University of Pennsylvania IRB protocol 833333; CCHMC IRB protocols 2020-0991).

Note that full information on the approval of the study protocol must also be provided in the manuscript.

Flow Cytometry

Plots

Confirm that:

☒ The axis labels state the marker and fluorochrome used (e.g. CD4-FITC).

☒ The axis scales are clearly visible. Include numbers along axes only for bottom left plot of group (a 'group' is an analysis of identical markers).

☒ All plots are contour plots with outliers or pseudocolor plots.

☒ A numerical value for number of cells or percentage (with statistics) is provided.

Methodology

Sample preparation	To obtain single cell suspension, mice spleen and/or lymphnodes were meshed in RBC-lysis buffer, washed by completed DMEM medium and filtered through 70µm strainer. For cellular staining, 1-2 million cell were stained at 4C for 15 min with Fixable Viability Dye (eBiosciences, 65-0863-14) and thenincubated with indicated antibody in DMEM medium supplemented with anti-CD16/21 for 30min at 4c.
Instrument	All flow cytometric analysis were performed by BD FACS-Canto .
Software	BD FACS-DIVA and FlowJo (ver 9 and 10, respectively)
Cell population abundance	FACS sorting was not used, and therefore cell population abundance not applicable.
Gating strategy	Cell were selected by scatter properties. Single cells were gated base on SSC-A/SSC-W. Dead cells were excluded by Fixable Viability Dye. CD45+ cells were gated on to gate out CD45- erythroid cells and non-leukocytes. B220+IgM+ cells were then gated followed by a gate on CD5 to identify B-1a cells. In some experiments, B10 cells were then identified based up expression of GFP under the control of the IL-10 promoter.

☒ Tick this box to confirm that a figure exemplifying the gating strategy is provided in the Supplementary Information.